INVESTIGATION OF FLOW CHARACTERISTICS OF IRON-ORE AND WATER SLURRY

A Dissertation

Submitted In Partial Fulfillment of the Requirement for the Award of Degree of

Master of Engineering

In

Thermal Engineering

Submitted by

SAGAR KUMAR

(ROLL NO. 801683024)

UNDER THE GUIDANCE OF

Dr. Satish Kumar

Associate Professor

DEPARTMENT OF MECHANICAL ENGINEERING

THAPAR INSTITUTE OF ENGINEERING AND TECHNOLOGY,

PATIALA

CERTIFICATE

I hereby declare that the thesis entitled "**Investigation of Flow Characteristics of Iron-Ore and Water slurry**" is an authentic record of my work carried out as for the award of the degree of Master of Engineering in Thermal Engineering at Thapar Institute of Engineering and Technology, Patiala, Punjab under the supervision of **Dr. Satish Kumar**, Associate Professor, Mechanical Engineering Department, Thapar Institute of Engineering and Technology, Patiala .

The matter presented in thesis has not been submitted for the award of any other degree of this or any other university.

Sagar Kumar

Date: 15/June/2018
Place: Patiala

Sagar Kumar
(801683024)

It is certified that the above statement made by the student is correct to the best of my/our knowledge and belief.

Dr. Satish Kumar
Mechanical Engineering Department
T.I.E.T, Patiala-147004

ACKNOWLEDGEMENT

First and foremost, I would like to give my sincere thanks to GOD, the Almighty, the source of my life and hope for giving me the strength and wisdom to complete the research work.

I would like to express my gratitude Dr. Satish Kumar, Associate Professor, Mechanical Engineering Department, Thapar Institute of Engineering and Technology, Patiala for his valuable guidance, support and for sharing his pearls of wisdom with me during my research work. Many times, his patience and constant encouragement has steered me to the right direction.

I am most grateful to Mr. Jashanpreet Singh and Mr. Jatinder Pal Singh for sharing their knowledge and all fruitful discussions on various aspects related to the basic concepts, experimental testing and testing instruments which helps me during the entire period of research work. I would also like to acknowledge my friend Mr. Mandeep Singh for his continuous support and encouragement.

I am also thankful to Dr. Vikrant Khullar, coordinator of Masters Program and to all other teaching and non-teaching staff members of Mechanical Engineering Department for providing me all the instruments required for carrying out my research work.

Last but not least I am always grateful to my family members for their unconditional support, encouragement and best wishes, without which I have not come this far.

(Sagar Kumar)

ABSTRACT

The rheological characteristics of uni-modal and multivariate iron-ore slurry have been examined. The study aimed to investigate the physical, chemical and morphological characteristics of iron-ore particles. Present study also includes the experimental investigation of flow characteristics of iron-ore slurry. The physical, chemical and mineralogical properties such as surface microstructure, chemical composition, crystalline phase analysis, particle size distribution (PSD), shape, static settled concentration, slurry density and pH of iron-ore were carried out prior to examination of rheological characteristics of iron-ore slurry. The surface microstructure was investigated by using Scanning electron microscopy (SEM) technique. The chemical composition was determined by using Electron dispersive spectroscopy (EDS) technique. The crystalline phases present in iron-ore particles were examined by using X-Ray Diffraction (XRD) technique. Particle size distribution of iron-ore particles was carried out by using British standard sieves. Bench-scale tests were performed to determine the density and static settled concentration of iron-ore slurry. The various parameters related to shape such as particle shape factor, sphericity and surface smoothness were determined by using numerical simulations. The simulations were carried out by digital interpretations by reading the pixel and grey value information present in a particular SEM micrograph. The iron-ore particles were found irregular in shape with knife edges. The circularity and sphericity of hematite iron-ore was lies in range 0.31-0.55 and 0.30-0.56 respectively whereas 0.34-0.51 and 0.36-0.54 respectively for magnetite iron-ore. The sphericity and circularity of iron-ore particles was found to be very low which indicated that particles of iron have irregular and conical shape. The pH value of uni-model and multivariate iron-ore slurry was lie in the range of 8.92 to 9.08. The experimental investigation of rheological characteristics of multiphase slurry has been devoted to understanding ability of material flow. The rheological experiments were conducted by using standard rotational rheometer (manufactured by: Rheolab Q-C, APC Ltd. Germany). The uni-modal sample of slurry was designated as sample S-1 and multivariate slurry sample was designated as sample S-2. The rheological experiments were conducted with varying solid concentration from 30 to 60% by weight. The uni-modal slurry exhibits almost Newtonian fluid flow-behavior up to the solid concentration of 30% by weight. However, in case multivariate slurry the flow behavior was found to be pesudoplastic at low concentration. Also, the apparent viscosity of slurry is highly influenced by the applied shear rate and the solid concentration. It has been noticed that the slurry

viscosity is very high at initial phase afterward it starts decreasing with further increase in shear rate. On the other hand, slurry viscosity increases with increase in solid concentration. The experimentation was further extended to study the effect of addition of finer particles on the rheology of uni-modal and multivariate slurry. The optimum reduction in viscosity was found at blending concentration of 30% by weight for the slurry of sample S-2 whereas, blending concentration of 20% by weight found to be optimum for the slurry prepared by sample S-2.

Keywords: Rheology, particle size distribution, bimodal, circularity factor, sphericity.

Table of contents

List of Figures

List of Tables

List of Symbols

τ	Shear Stress, Pa
μ	Viscosity. Pa.s
$\gamma, \frac{du}{dy}$	Shear rate. 1/s
n	Flow index
k	Flow parameter
λ	Wavelength, m
d	Lattice distance
m	Reflection order
C_1, C_2	Form factors
r_i	Inner radius, m
r_o	Outer radius, m
r_a	Average radius, m
H	Height of cylinder, m
C_w^{max}	Maximum settled concentration
σ	Specific gravity of slurry
Φ	Sphericity of particle

Chapter 1

Introduction

Mining is considered as an endeavor of humankind granted agriculture. Both industries considered as basic or primary industries of the ancient civilization. Although, if we consider fishing, lumbering and agriculture as one part, procuring and processing of oil and gas with mining similarly, then agriculture and mining are the primary source to fulfill all the basic needs of past and present civilization. From prehistoric time to present, mining industry plays crucial role in the advancement of human existence (Madigan1981). The term *mining* here is used for the extraction of naturally occurring mineral matters such as solids, (ores i.e. iron, aluminium, zinc, coal etc.) liquids, (petrochemical products such as gasoline) and gases (natural gas etc.) from the earth's crust or heavily bodies for utilitarian purposes.

The mining history is interesting and move parallel with the history. Also, many important cultural eras and advancements are allied with it and considered by many minerals or their derivatives as period prior to 4000 B.C.E recognized as Stone Age, period about 4000 to 5000 B.C.E known as the Bronze Age, the time from 1500 B.C.E to 1780 B.C.E starting period of human development called Iron Age, the period of iron derivate from 1780 to 1945 identified as Steel Age and Nuclear Age the time after the World War-II i.e. from 1945 to till now. Various mileposts of human history such as journey of Macro Polo's to China and Vasco da Gama's expeditions of India as well as Africa, the discovery of New World by Columbus and the modern gust toward gold that lead to the establishment of California, Australia, Alaska, South and North America were attained with mineral providing a major incentive (Rickard 1932). Some other remarkable and stimulating facts about the history of mining and metallurgical industry also reported in the historical records of Gregory (1980), Raymond (1984).

Mining industry plays a vital role in every aspect of development it may be social, economic and industrial development. The increase in population and advancement in technology is also increasing the demands of raw material for industry which results in increase of mining operation. Now-a-days, mining industry contributes almost in every field such as agriculture, transportation, construction, energy, health etc.

1.1 Iron-ore

Minerals are extracted from the earth's crust and from heavy rocks. Usually, minerals are founded in the form different chemical compounds in nature which is generally known as ore. The earth crust contains nearly 5% of iron naturally and it is one of the most abundant elements in earth's crust which is being used extensively from 6000 years approximately. Also, iron is a building block of industrial revolution as it is one of the cheapest and strongest metals. Australia, Brazil, India and China are the largest producers of the iron-ore in globe. Magnetite and Hematite are the richest source of iron however the extraction of iron from carbonates and sulphide ores is not economical. In India, hematite ore is found in Madhya Pradesh, Jamshedpur, Madras, Mysore, Noamondi, etc. whereas magnetite is found in Mysore, Salem and Trichinopoly. Siderite is found in Raniganj (West Bengal).

1.2 Classification of Iron-ore

Metallic iron is extracted from its ores. The iron-ores are available in the form of oxides, carbonates or sulfides and colours vary from bright yellow, deep purple, rusty red to dark grey. Iron-ores are the basic raw material in the production of steel which is approximately 98% of the total iron extracted in the world. The major types of iron-ore which are widely used for the extraction of iron are shown in Fig 1.

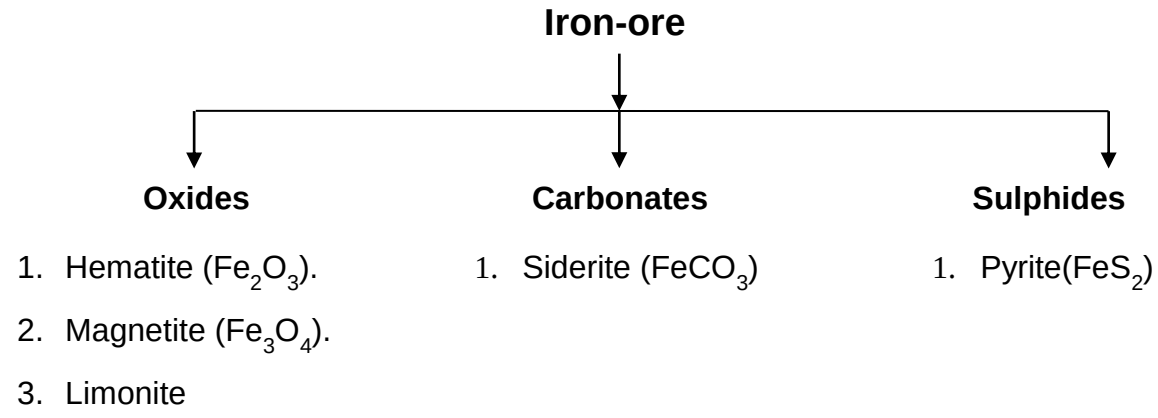

Figure 1.1 Different types of iron-ore

a) **Hematite (Fe_2O_3):** Hematite ore is oxide ore which contain rich amount of iron nearly 68-70%. In India, hematite ore is widely used for the production pig iron. Hematite ore has relative high density as compare to the gangue material like silicates and carbonates associated with it, also combination of beneficiation techniques are used for separation.

b) **Magnetite (Fe_3O_4):** Magnetite is also oxide of iron which is also enriched with iron content approximately 72-75%. Due to its magnetic behaviour, it can be easily separable from the unwanted material. The ore is found in the form of small rocks and irregular in shape.

c) **Limonite ($Fe_2O.\ nH_2O$):** It contains 60% of iron. It is a hydrated oxide of iron usually forms from hydration of hematite and magnetite. It is amorphous in nature and some called as bog iron-ore.

d) **Siderite ($FeCO_3$):** The deposit of siderite or spathic iron-ore usually, covered with rusty capping. Nearly 35-40%of iron content is present in siderite ore. It is available in crystalline structure. In order to remove carbonate content ore is first roasted. Iron obtained from this ore is of very low quality.

e) **Pyrites (FeS_2):** Approximately equal amount of iron content is present as in siderite. Iron obtained from the ore is also of low quality and high in sulphur content. Similarly, roasting is done to remove the sulphur from the ore.

1.3 Applications of iron-ore

Minerals ore such as iron, aluminium, zinc and lime are unevenly distributed in the earth's crust. Ore extracted from mines first crushed to small particles as it is difficult to extract mineral directly from mine output as extracted material contained many unwanted materials. After crushing, the various mechanical separation techniques are used to separate the mineral and macro-material from the ore. Iron also play vital role in the development of country's economy and the standard of living. The pure iron is easily magnetized and melts approximately 1530^oC. Ukraine, Russia and Brazil are the largest producer of iron-ore. Australia, USA, China, South Africa, India also contributed in the production of iron. Iron-ore has wide application in our day-to-day life as some of basic applications of iron-ore are listed below:

- Initially, the extracted iron from ore is transformed in to pig iron which is further used in the production of steel. As 98% of world's iron-ore is used to make steel, it is about 90% of total metals used in whole world.
- Steel properties like high strength and high corrosive resistant make it suitable for manufacturing many different sophisticated instrument and machine parts such as pipes, cars, ships and engine and aeronautical machines parts etc.
- Although cast iron, wrought iron and layered iron auxiliary sheeting are conspicuous material in building development.
- Magnetite ore is used to evacuate impurities from the coal and magnetic property makes it reusable.
- Iron is also a good reducing agent, hence used in many chemical reactions as catalyst to increase the reaction rate.

1.4 Transportation of iron-ore

The growth of country heavily relies on the industrial development in country. Unfortunately from last few decades, the mining industry causes very much disturbance to the environment. The major damage to the environment because of iron-ore mining and transportation is the declining the quality of air. Also, the transportation of minerals from mining site to mineral processing industry plays a crucial role. To fulfill the increasing demand of minerals, it is necessary that raw materials reached on right time. The major ways of transportation of iron-ore are rail, road, ports and the slurry pipelines.

1.4.1 Slurry pipelines

A slurry pipeline is an alternate way of transporting the mineral ores such as coal, iron-ore and mining waste called tailing, over the long distance (Yuchi *et al.*, 2005; Bobicki *et al.*, 2013). The concentrate mixture of ore and water is pumped over a long distance to ports and mineral processing industries for the further processing. In processing industries the material is separated from the slurry with the help of filter press or gravitational settling method, in order to remove water. In recent years, the use of pipeline to transport the bulk solid is very common in many industries (Tangsathitkulchai, 2003; Singh *et al.*, 2016).

1.4.2 Need of slurry pipeline

- To fulfill the increasing demand of iron and coal for industry, it is necessary to find the alternate of present mode of transportation.
- As road and rail are not capable modes, as these modes are already very much burdened. However, the roads and rail are also not capable for transporting fine ore concentrate.
- The transportation of iron-ore through rail and road also not guarantee to deliver frights on time.
- The transportation of iron-ore through rail and road cause environment pollution.
- The cost of logistics is 12-13% approximately of GDP against 8-10% in developed world.
- Also, the pace of infrastructure development is not matching with industry's requirement.

1.4.3 Benefits of transportation of iron-ore through slurry pipeline

- Bulk transportation of iron-ore through slurry pipeline does not cause any noise, smoke or air pollution hence it is very environment friendly.
- Ore can be transported to short as well as long distance. Usually transportation of ore from remote areas and mountains is done with the help of slurry pipeline.
- As slurry surface condition such as storm and inclement in weather has no effect on pipeline, ore can be transported throughout the year.
- It also reduces the burden on the other transport mode such as rail and roads.
- Transportation of ultrafine ore requires special wagons, which can be easily avoided by slurry transportation mode.
- Due to its easy construction, low operational and maintenance cost make it very much effective as compare to the other mode of transport.

1.4.4 Factor affecting slurry transportation

During transportation of solid-liquid suspension, the properties of slurry are highly influenced by particle size, slurry viscosity, solid concentration, shape of solid particles. Since, it is mandatory to study the rheological properties and morphological properties of solid-liquid suspension so that slurry transportation system should be operate at higher efficiency (Singh, Kumar and Mohapatra, 2017). Mineral suspension is broadly divided into two categories: settling slurries and non-settling/slow settling slurries (suspension slurries). The minerals

suspension constitute fine particles settled at slow rate which means that rheological properties can be measured using generic standard rheological instruments whereas slurry consists of heavy particles settled very fast, hence the rheological characteristics of these slurry can investigate in standard instruments including: capillary tube, parallel plate, bob and cup.

1.4.5 National and International scenario of iron-ore slurry pipeline

Table 1.1 National and International scenario of iron-ore slurry pipeline. ('Slurry Tranportation in Indian Mines', 2001)

Sr. No.	National scenario	International scenario
1.	Kudremukh to Mangalore , KIOCL, 68 Km, capacity 8.0 Mt/yr	Savage River , Tasmania , Australia, 85 Km
2.	Kirandul (Baildaila Sector) to Vishakhapatnam Essar Steel , 267 Km, capacity 8.0 Mt/yr	Wellstead to Albany port, Australia, 100 Km
3.	Barbil to Kalinganagar, BRPL,Orissa, 230 Km, capacity 4.0 Mt/yr	Mount Gibson Ranges to Geraldton, Asia Iron Holding, Australia, 278 Km, capacity 10 Mt/yr
4.	Joda (Dabuna)- Paradip, Orissa, Essar Steel, 253 Km, capacity 8Mt/yr	Balla Balla Mines to Port Hedland, Aurox Resources, Australia 110 Km, capacity 10 Mt/yr
5.	Mangalore to Tornagallu: 350 Km by JSW (Advance stage of implementation) both for ore/coal, investment Rs 2100 crores	Samarco : from Germano to Point Ubu Pellet Plant in Brazil, 396 Km, capacity : 15Mt/yr.
6.	Kirandul –Bacheli – Nagarnar - Vizag , NMDC 455 Km , capacity 10 Mt/yr (Ongoing project)	Minas Gerais to Iiheus Port, Brazil, 420 Km, capacity : 25 Mt/yr

The Kirandul- Vishakhapatnam slurry pipeline is second largest pipe in world and has drastically reduce the cost transportation from Rs. 550 per tonne to merely Rs. 80 per tonne.

1.5 Rheology

Fluid is a substance that undergoes infinite deformation under the influence of applied force. Rheology delineates as the study of movement of matter, generally in aqueous state, or as 'soft solid' i.e. solid that undergoes plastic flow under the influence of realistic force and remained deformed under certain condition (Morrison, 2001; Antony N. Beris, 2014). In other words, it is defined as study of fluid behavior under the influence applied force. However, on fluid only normal compressible and shear stress can be applied whereas in rheology generally study of fluid behaviour is done under the influence of applied shear stress. Usually two plate model is used to study the behaviour of fluid. The schematic diagram of two plate model is shown in **Figure 1.2**.

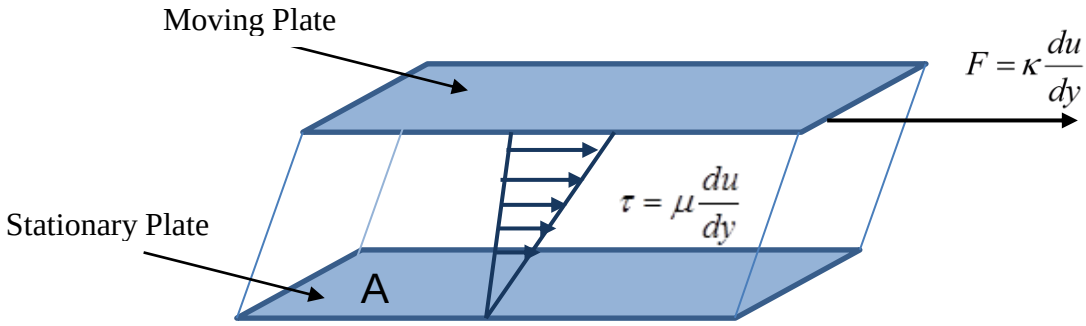

Figure 1.2 Parallel plate model of deformation of fluid under an applied force

Flow is defined as continuous irreversible deformation due to internal and external friction offered to the flowing matter. The internal friction to the flow is called as viscosity and denoted by μ. Viscosity (internal friction) is defined as the property of a fluid which offers resistance to the movement of one layer over another layer of the fluid and called as cohesiveness of fluid in layman language. Under the effect of applied shear force, each layer of fluid would movie with different velocity depending distance from the plane of applied force. Shear strain $\gamma = \frac{du}{dy}$ is also known as velocity gradient which is perpendicular to the plane of applied stress. According to the Newton's law (Kissa, 1999),

$$\tau = \mu \frac{du}{dy} = \mu\gamma \tag{1.1}$$

The fluid which obeys the Newton's law is termed as Newtonian fluids having constant viscosity (μ). However in non-Newtonian fluids, the viscosity of the fluid depends upon of shear rate and shear stress. The slope of plot between the shear rate and the shear stress indicate about the type of fluid. As in case of Newtonian fluid, the slope of the graph is straight line whereas non-Newtonian fluid is further categorized based upon the shape of the curve reflects the category of the flow. The shapes of slope for different types non-Newtonian fluid is shown in **Figure 1.3**.

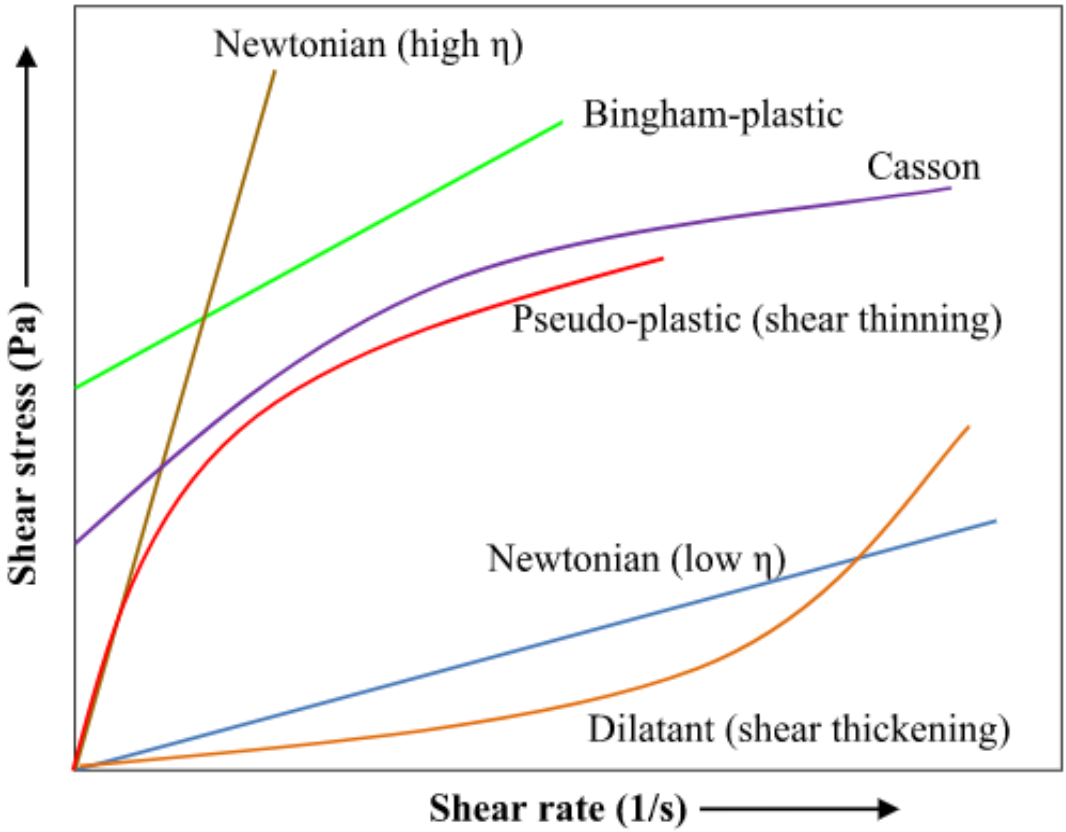

Figure 1.3 Rheograms of different fluid models (WANG *et al.*, 2009).

1.6 Different Rheological models

Rheology describes the trends of non-Newtonian fluid by determining the parameters required to develop relationship among the deformation rate and shear stress. The shape of curve reflects the category of the flow. In order to determine the various parameters, the different rheological models are used. The majorly used rheological models are listed in **Table 1.2**.

Table 1.2 Various rheological models with model equations

Type of non-Newtonian fluid	**Model equation**	**No. of parameters relating shear stress and shear rate.**
Bingham Law	$\tau = \tau_y + \mu\gamma$	Two parameter
Power-Law	$\tau = k\gamma^n$	Two parameter
HERSCHEL -Bulkley	$\tau = \tau_y + \mu\gamma^n$	Three parameter
Casson	$\tau^{1/2} = \tau_y^{1/2} + (\mu\gamma)^{1/2}$	Three parameter

Two parameter rheological models are widely used to study the fluid flow behaviour. As Bingham model is used to study the flow behaviour of petroleum drilling fluid and many different type muds whereas Power law is used study the rheology of soft solid such as coal and ash slurry. Casson model is used for visco-plastic fluids which have wide application to model the flow of blood. Similarly, Herschel-Bulkley is used to study the rheology of slurry formed by hard solids such as iron-ore but all of above mentioned models have been found a good approximation for other fields like rheology of food product and polymer etc.

1.7 Importance of rheology

- Rheology helps to estimate about mixability and pumpability of the iron-ore slurry which helps in designing of iron-ore slurry transportation system.
- Rheology also helps evaluate the frictional pressure drop when iron-water slurry flows in pipes.
- Rheology evaluates the ability of slurry to transport the fine and large particles. It also studies the effect of surrounding temperature on the flow behaviour of suspension of iron.
- Rheological data is also very important to find relationship between the pump and flow in pipelines. It also helps us in selecting pump of enough power so as to transport slurry to the distance.
- Rheological data is primary raw data which is required for the the computational analysis of slurry flow.

Chapter 2

Literature Review

2.1 Literature Review

A lot of research has been done by many researchers on the rheology of the slurry suspensions, which set foundation for the present investigation. Several factors that contribute in altering the rheological behavior of mineral slurry has been investigated by researchers and an optimum value that promotes an economic slurry transport with an appreciable viscosity in a particular shear rate range has been found.

Yavuz et al. (1998) investigate effect of particle size on the rheology of lignite - water slurry. The procured sample of lignite was sieved into six different particle sizes: <45, 45 - 53, 53 - 63, 63 - 75, 75 - 90, 90 - 125 μm. Rheology experiments were performed at solid concentration of 60% by weight at room temperature (i.e. 20°C). They delineates that the finer particles had high viscosity value which is not suitable for the transportation of slurry at higher concentration. However with the blending of courser particle (90-125 μm), viscosity of lignite slurry was improved.

Ghanta et al. (2002) study the influence of particle size distribution, concentration and surface properties by taking coal and copper ore slurry. They found that viscosity of coal slurry suspension is reduced with increasing particle size of coal, whereas in case of copper ore as particle size increases viscosity. They also observed that rheology of fine particulate slurry suspension improved with the addition of coarse particle of ash.

He et al. (2004) performed an overview about the experimental studies conducted by previous researchers on rheology of ultrafine grinding of industrial minerals. They summarized the work of previous researchers used to modeling rheological behaviour of slurries and the techniques for the characterization of the suspension. The semi-empirical model including slurry rheology, solids concentration, and particle size and slurry temperature was described. They reported that the different parameters such as particle size, solid concentration and distribution, particle shape temperature and pH affects the rheology of the slurry prepared by ultrafine grinding of industrial minerals.

Yang and Aldrich (2005) performed experimentation in the presence of magnetic field on aqueous suspension of magnetite ore particle size of 75 μm to investigate the flow behavior. They reported that non-magnetized slurry above 30% solid concentration by weight exhibit Bingham plastic behavior whereas when the slurry suspension exposed to external magnetic field of 41×10^{-4} T, the flow behavior can be described by Herschel-Bulkley with flow index (n) range from 0.38 to 0.9.

Yuchi et al. (2005) performed a study on multivariate regression analysis of sixteen samples coals procured from various mines of China with different ranks of coal vary between lignite to anthracite to find the correlations between eighteen different parameters from forty coal properties. They found that the carbon content and grindability index of coal shows positive relation with the slurryability while content of moisture present in air at equilibrium and surface area found by mercury porosimeter results in negative impact. The rheological behavior of coal water slurry related positively with ash content, soluble ions, and volume of pore examined by Mercury porosimeter while zeta potential properties of surface of the coal impacts negatively on the rheological behavior of coal water slurry.

Roy and Das (2008) studied the effect of geochemical and mineralogical characteristics on beneficiation process of low grade iron ore sample procured from Bellary-Hospet sector, India. They found that the major gangue elements are goethite, magnetite and limonite present in small amount. However, the Electron microscopic studies revealed that the size of gibbsite grains varying from 10 to 50 microns and associated with the iron phase. The geochemistry data show adverse relation of Fe_2O_3 with silica and alumina. They stated that if the particle size of gangue material is too fine as compare iron oxide then magnetic separation method is best but if the size gangue material and ore particles are too fine flotation in general and flotation in column in particular situation seems to be more effective.

Senapati et al. (2009) studied the rheological behaviour of lime-water slurry at different solid concentration (by volume), particle size and slurry temperature. They reported that the shear stress is a direct function of shear rate and behaves as almost Newtonian fluid for the solid concentration below 30% by weight beyond which slurry was highly pesudoplastic in nature. They also stated that viscosity of limestone mineral slurry decreases with temperature

and the change can be explained by Arrhenius equation in terms of required activation energy.

Zhou et al. (2010) performed an experimental study on concentrated suspension of coal water slurry to investigate the rheological behaviour. They prepared slurry from Datlong coal using Haake rheometer and performed a regression analysis on experimental data to fit different rheological models. They found that the aqueous suspension coal-water at solid concentration of 60 and 70% (by weight) exhibit pseudoplastic behavior. Also, the experimental data found to be well fitted with two variable rheological model Herschel-Bulkley.

Agudo and Navarro (2010) examined the flow and the morphological characteristics of lime putties acquired after hydraulic treatment and compared different morphological parameters and flow behavior. They found that behaviour of hard burnt lime and lime putty is non-Newtonian and fluid is rheopectic in nature. Improved reheological behaviour was achieved after hydro-treatment of the hard burnt lime whereas lime putty become more reactive after the treatment due to smaller particle size and large surface area.

Deosarkar and Sathe (2012) studied theoretical models to investigate the impact of various factors used for predicting viscosity of magnetite-water suspension. Models were fitted to experimental data of rheology of magnetite ore up to solid concentration of 30%. Slurry samples were prepared by using different particle size of solid such as 53, 52.3, 58.4 and 74.8 μm. The rheogram data to predict effective viscosity of the slurry was best fitted to Liu's model amongst all six models tested for the prediction. Also, the prediction done by using ANN model between the slurry parameters and effective viscosity were found more close to the experimental data.

G. Vieira and E. C. Peres (2012) studied the effect twenty different additives on the rheological behaviour of concentrate iron-ore water slurry. They reported that slurry exhibit pesudoplastic behaviour and flow behaviour can be explained by Herschel-Bulkley and Bingham model. They found at the dosage 300 g/t: polyacrylic acids (DPW 410, DPW 510, and DPW 610), citric acid, and sodium hexametaphosphate promoted reduction of the fluid consistency index and the plastic viscosity. Whereas, further increase of dosage to 600 g/t and 900 g/t did not result in significant change in the flux curves.

Vieira and Peres (2013) investigated the effect of regrinding of iron-ore concentrate on dispersion and rheological characteristics of slurry. The regrinding tests were performed under different pH value i.e. 7.3, 8.5 and 10.0 of dispersion with the addition of lime at concentration of 300 g/t. The degree of the slurry dispersion increases as pH vary from 7.3 to 10.0, but the values of yield stress and apparent viscosity noticed to be lower, and the specific energy consumption reduced by 17.4%.

Vance et al. (2013) studied the impact of addition of lime, fly ash and metakaolin on the flow properties of cement pastes. A Bingham model of rheology was used to predict the flow behavior of the paste. They delineate that plastic viscosity and static stress of the slurry remain unchanged. However, if the ordinary portland cement (OPC) replaced by coarse lime powder results in decrease in yield stress and plastic viscosity of slurry mixtures.

Trahana et al., (2014) performed experimentation on air-rock bed thermal energy storage system to examine the effect of pressure drop and particle sphericity. They investigated the pressure drop characteristics of packed bed thermal energy storage system by taking irregular shaped solid particles and keep the ratio of tank to the diameter of particle constant i.e. 10.4. From experimental data, they derived an empirical relation to predict the pressure losses in bed of irregular shape particles.

Walker and Hambe (2015) observed that the wear rate during the transportation of slurry is highly influenced by shape factors such as circularity factor and spike parameter on the erosion wear of the material through image processing. They concluded that the shape of the particle for wear purposes can be characterized by the circularity factor. They found linear relationship between circularity factor and the spike parameter for wide range particles shapes and inverse power law relationship between circularity factor and wear rate.

Assefa and Kaushal (2015) investigated the rheological properties of coal ash slurry at high concentration ranges from 50-70% (by weight). They proposed an model from experimental results by considering viscosity as dependent variable while solid volume fraction, mean particle diameter and coefficient of uniformity as independent variable and also, use nonlinear least square method for optimization. They concluded that the proposed model shows close agreement with experimental data and able to predicted viscosity of multi-sized Bingham slurries at higher concentration.

Sahoo, De and Meikap (2015) investigated the effect of microwave energy, slurry concentration and particle size distribution on iron ore-water slurry. They carried out the microwave pretreatment of iron ore for rheological experiments for 30, 60, 90 and 120 seconds. They found that the viscosity of slurry increases with sold loading and particle size whereas the slurry prepared after the microwave treatment of iron ore exhibit better rheological characteristic as compared to slurry prepared by without microwave treatment and slurry prepared in all cases exhibit shear thinning and pesudoplastic behaviour. Also, the specific gravity of microwave treated iron ore slurry is less as compared to slurry prepared by untreated iron ore.

Singh et al. (2016) studied the effect of particle-size distribution and temperature on rheological behavior of coal slurry. They found that the rheological behavior of slurry suspension of finer particles (<53 μm) is highly influenced by the addition of coarser particles (53-75 μm, 106-150 μm and 150-250 μm). They reported that apparent viscosity of coal water slurry is decreased with particle size and temperature. Also, the slurry viscosity decreased with addition of coarser particle upto some extent and the optimum fraction was found to be 30% (by weight) in slurry.

Liu et al. (2017) delineated some critical improvement in morphology analysis of volcanic ash. They used different shape techniques for the measurement such as (2-D) two dimensional cross-sectional imaging, projected area images and also discussed their applications. They found four different parameters namely – solidity, axial ratio, convexity and form factor. They found that ash particles have wide range of solidity factor varying from 0.71-0.83.

Liu et al. (2017) performed experiment on biochar-water slurry fuels to investigat the effect of particle size and particle size distribution on the yield stress, viscosity and stability of the slurry. It was found from the experimental results of a biochar-water slurry fuel that with increase in for D_{50} < 15 μm, the yield stress decreased slightly but when median particle size D_{50} was larger than 15 μm the yield stress increased sharply, due to an increase in the water uptake capacity. The viscosity of bimodal size distribution of sized slurry was found to be less than that of the slurry prepared by the unimodal size distribution biochar. The viscosity a

biochar slurry fuel of bimodal particle size distribution increased as the ratio of coarse to fine fraction in slurry increased, being more profound at smaller fine fraction particles.

Kumar et al. (2017) carried out an experimental investigation to analyze the rheology of bottom ash-water slurry with/without additives. They had taken Henko detergent and sodium sulfate as an additive. They found that the reduction in apparent viscosity is highly noticeable with addition of additives in bottom ash suspension in range of 0.2-0.6% at solid concentration of bottom ash suspension was taken in range of 10 to 60% (by weight).

Nyembwe, Cromarty and Garbers-Craig (2017) delineate the relationship between granule shape, permeability and granulation mechanisms for the production of sinter. They found that four basic mechanisms governed the formation of granules namely coalescence, adhesion in micropellets and layering in two stage. However, the addition of iron ore promotes the mean sphericity of the granules while decreasing the sinter bed voidage and permeability.

Table 2.1 Tabulated summary of literature review

Authors	**Year**	**Flowing media**	**Observations**
Yavuz et al.	1998	Lignite water slurry	They conduct an experimental study on six different particle size of lignite water slurry at solid concentration 60% by weight. They found that fine particles have higher viscosity and are not suitable for transportation but can be transported after blending with coarser particles (i.e. 90-125 μm).
Ghanta et al.	2002	Coal and copper slurry	They performed an experimental study to investigate the rheology of coal and copper slurry. They found that viscosity of coal slurry decreases with increase in particle size. However, in case of copper ore slurry the viscosity of slurry increases with increase in particle size.
He et al.	2004	Industrial minerals	They summarized the experimental work of previous researcher on ultrafine industrial minerals. They conclude that the rheology of slurry was affected by various parameters such as particle size, solid concentration, pH, Particle shape and temperature.
Yang and Aldrich	2005	Magnetite ore-water slurry	Aqueous suspension of magnetite ore exhibit Bingham plastic behaviour above 30% solid concentration by weight. In the external magnetic field slurry exhibit shear thinning behaviour and can defined by Herschley-Bulkley model with flow index lies between 0.39 to 0.9.

Yuchi et al.	2007	Coal-water slurry	The carbon content and grindability index of coal improved the slurryability coal water slurry. Whereas air equilibrium moisture and surface area determined by mercury porosimeter gave negative effects
Roy and Das	2008	Iron-ore	They investigated the geochemical and mineralogical characterization of low grade iron ore sample collected from Bellary-Hospet sector, India and their implication on beneficiation process. They found that the major gangue elements are goethite, magnetite and limonite present in small amount and magnetic separation technique is best in order to separate the fine gangue particles
Senapati et al.	2009	Limestone slurry	They reported that slurry exhibit Newtonian behavior up to a 30% concentration beyond which slurry was highly pesudoplastic in nature. The viscosity of limestone mineral slurry decreases with temperature and the change in viscosity can be explained by Arrhenius equation.
Zhou et al.	2010	Coal-water slurry	They found that the aqueous suspension coal-water at solid concentration of 60 and 70% (by weight) exhibit pseudoplastic behavior. Also, the experimental data found to be well fitted with two variable rheological model Herschel-Bulkley.
Agudo and Navarro	2010	Lime putties	They examined the flow and the morphological characteristics of lime putties acquired after hydraulic treatment and compared different morphological parameters and flow characteristics. They found that behaviour of hard burnt lime and lime putty is non-Newtonian and fluid is rheopectic in nature

Deosarkar and Sathe	2011	Magnetite ore-water slurry	Models were fitted to experimental data of rheology of magnetite ore up to solid concentration of 30%. Slurry samples were prepared by using different particle size of solid such as 53, 52.3, 58.4 and 74.8 μm. The rheogram data was best fitted to Liu's model among all six models tested to predict the slurry effective viscosity. Also, the relationship between the slurry parameters and effective viscosity found by ANN model were found more close to the experimental data.
G. Vieira and E. C. Peres	2012	Iron-ore water slurry	They reported that slurry exhibit pesudoplastic behaviour and flow behaviour can be explained by Herschel-Bulkley and Bingham model. They found five reagents promoted reduction of the fluid consistency index and the plastic viscosity at the dosage 300 g/t: three polyacrylic acids (DPW 410, DPW 510, and DPW 610), citric acid, and sodium hexameta phosphate. The dosage increase to 600 g/t and 900 g/t did not change significantly the flux curves.
Vieira and Peres	2013	Iron-ore water sluury	Regrinding tests were conducted under different conditions of dispersion (pH 7.3, 8.5 and 10.0) and with the addition of 300 g/t of lime. The increase of pH from 7.3 to 10.0 increased the slurry dispersion degree, providing lower values of yield stress and apparent viscosity, and a reduction in specific energy consumption of 17.4%.
Assefa and Kaushal	2015	Fly-ash and Bottom-ash slurry	They performed regression analysis on experimental data using an empirical rheological model for viscosity as a function of solid volume fraction, mean particle diameter and coefficient of uniformity and optimized. They concluded that the model shows close agreement with experimental data and able to predicted viscosity of multi-sized Bingham slurries at higher concentration.

Sahoo and Meikap	2015	Iron-ore-water slurry	They found that apparent viscosity of slurry increases with slurry concentration and particle size whereas the slurry prepared by microwave treated iron ore exhibit better rheological characteristic as compared to slurry prepared by untreated iron ore and slurry prepared in all cases exhibit shear thinning and pesudoplastic behaviour. Also, the specific gravity of microwave treated iron ore slurry is less as compared to slurry prepared by untreated iron ore.
Singh et al.	2016	Coal-water slurry	The rheological behavior of slurry suspension of finer particles (<53 μm) is highly influenced by the addition of coarser particles (53-75 μm, 106-150 μm and 150-250 μm). They reported that apparent viscosity of coal water slurry is decreased with particle size and temperature. Also, the slurry viscosity decreased with addition of coarser particle up to some extent and the optimum fraction was found to be 30% (by weight) in slurry.
Kumar et.al.	2017	Bottom-ash	They had taken Henko detergent and sodium sulfate as an additive. They found that the reduction in apparent viscosity is highly noticeable with addition of additives in bottom ash suspension in range of 0.2-0.6% at solid concentration of bottom ash suspension was taken in range of 10 to 60% (by weight).
Liu et al.	2017	Volcanic ash	They delineated some critical improvement in morphology analysis of volcanic ash. They use different techniques for the measurement of the shape techniques including cross-sectional (2-D) imaging, projected area images and discuss their applications. They found four different parameters namely – solidity, convexity, axial ratio, and form factor. They found that ash particles have wide range of solidity factor varying from 0.71-0.83.

Liu et al.	2017	Biochar slurry	The viscosity of a slurry fuel prepared using biochar of a bimodal size distribution was less than that with a unimodal size distribution. The viscosity of a slurry fuel prepared using a biochar of bimodal size distribution increased as the size ratio of coarse to fine fractions increased, being more profound at smaller fine fraction contents.
Nyembwe et al.	2017	Cement paste	They delineated the relationship between granule shape, permeability and granulation mechanisms for the production of sinter. They found that four basic mechanisms namely coalescence, adhesion in micropellets and layering in two stage permotes the formation of granules. However the addition of iron ore promotes the mean sphericity of the granules while decreasing the sinter bed voidage and permeability.

2.2 Gaps in Literature

The literature review conducted in above section revealed many hidden layers of gaps in terms of flow behaviour of mineral ore slurries. Following gaps of knowledge are observed from the reviewed literature as below:

- Empirical correlations developed experimentally for prediction of the rheology are applicable to particular slurry and cannot predict reasonable rheology with other slurries.
- At present time, different industries are using additive mixed slurries so, limited database is available in literature in terms of slurry-additive mixture. Limited investigation on rheology of minerals has been carried out with additives and stabilizers.
- Due to incomplete understanding of complex solid-liquid suspension and limited data base, there is limited established method available to predict the rheology for solid–liquid mixtures.
- Limited literature reports the effect of multisized particles on the rheological characteristics of mineral ore slurry.

2.3 Objectives

The objectives of this work are focused to investigate the physical, chemical, morphological and rheological characteristics of iron-ore and suspension of iron-water. The limitations of available experimental data and correlations have motivated the author to undertake the present study. The efforts of the present study will be to:

- Investigate the physical and chemical characteristics of two different ores of iron such as hematite and magnetite.
- Investigate the effect of solid concentration on the rheology of mineral suspension. The flow behaviour of slurry was highly affected by concentration of solid present in slurry which effect the specific energy consumption required for transporting the slurry.
- Analyze of rheological/flow behaviour of ore-water slurry as a function of temperature: A comparative study of uni-modal, bi-modal, and tri-modal particle size distributed slurries.

First objective: We want to determine the physico-chemical characteristics of iron-ore. However in order to investigate the morphological and chemical characteristics of iron-ore suitable experiments will be performed. In order to analyze the shape of particles scanning electron microscope will be used and further post processing tools were used to analyze the images obtained from scanning electron microscope, various factors related to shape of the particles will be determined. In order to examine the chemical composition by using energy dispersive spectroscopy and X-ray diffraction of samples will be done.

Second objective: During transportation of slurry or solid-liquid mixture the flow characteristics of slurry is highly influenced by the concentration of solid present in slurry. For this we will need to choose and perform suitable rheological experiments. We will conduct rheological experiments using rotational rheometer with varying amplitude of shear rate at different solid concentration. As a second step is to fit the experimental data on different rheological model in order to determine the best suitable model that can define the flow behaviour of slurry.

Third objective: In the extension of flow study, the first objective is to characterize the iron-ore by means of various techniques. Further in next step, we study the flow behavior of iron-ore slurry at different solid concentration. After successfully achieving first objectives, the effect of blending and temperature on the flow characteristics of iron will be investigated.

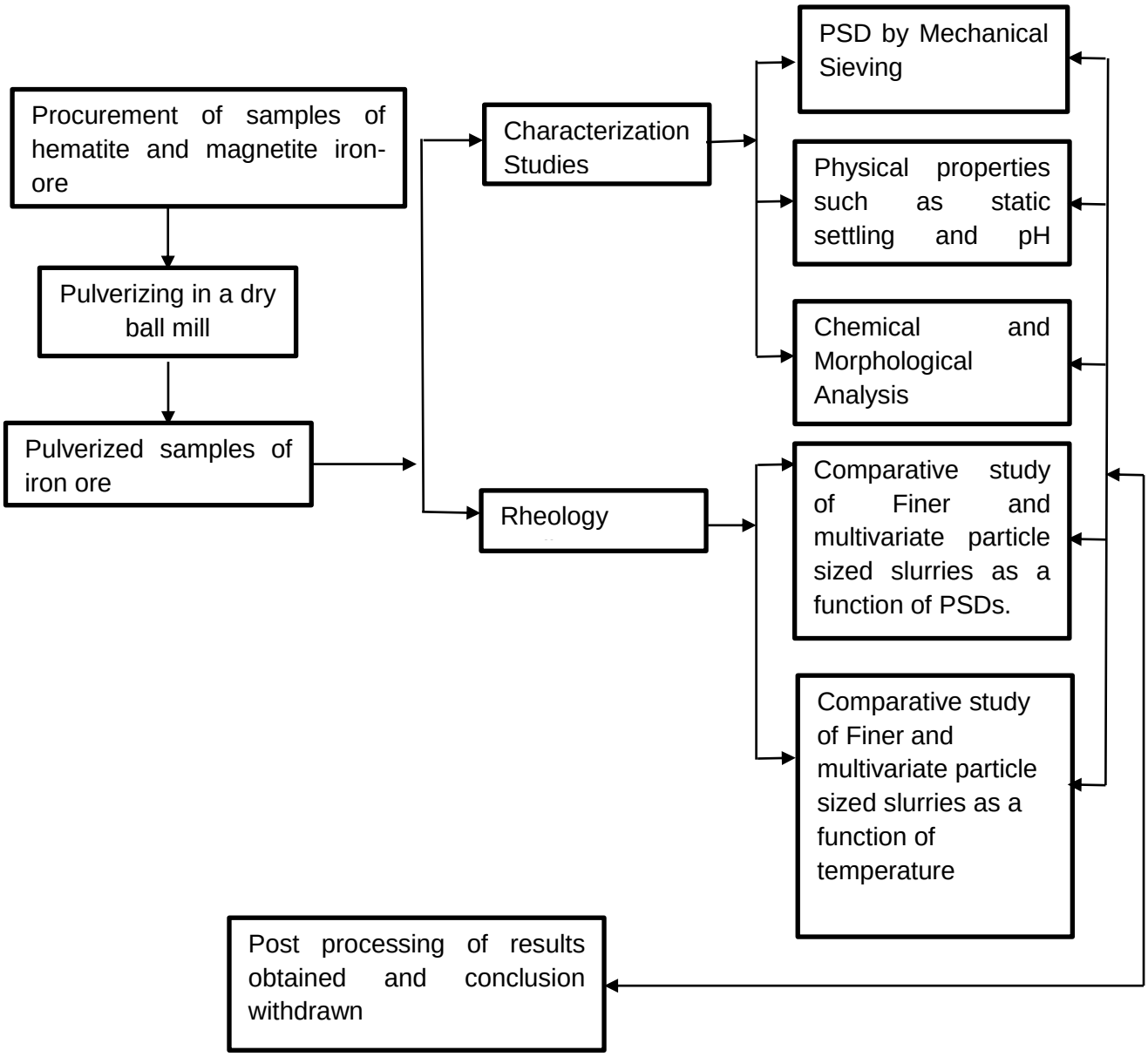

Figure 2.1 Flow chart of work

Chapter 3

Materials and Methods

This chapter includes the different techniques used to characterize the particle and suspension physical properties. The method used for the preparation of sample for experimentation is discussed. The procedure for measuring flow properties is included. The preparation of slurry and test methods for particle size, shape of particle and chemical composition are also included.

3.1 Particle Size Distribution (PSD)

The assortment in the size of the particles in specimen and the amount of particle present in varying size ranges were calculated in order to obtain particle size distribution. In order to remove the moisture from the sample, a known weight of sample was placed in to the oven at 120^0C for 30 minutes. An oven dried sample was considered and pounded on British Standard sieve. A mechanical sieve shaker (at Sand Testing Lab, T.I.E.T., Patiala) was used for sieving with sieves of size 1000, 710, 500, 355, 250, 150, 106, 75, and 53 μm, as shown in Figure 3.1. The mass retained on the each sieve was carefully collected, represent in percentage.

Figure 3.1 British standard mechanical sieve shaker

3.2 Scanning Electron Microscopy (SEM) / Energy Dispersive Spectroscopy (EDS)

Scanning Electron microscopy and Energy Dispersive Spectroscopy are widely used to study the surface and chemical properties of almost all types of materials. Both of analyses were done on same machine as equipment required for testing are mounted on one machine. SEM is commonly used to study the surface characteristics of the specimen. The micrographs obtained from the SEM are much easier to interpret. The instrument used for testing was SEM-JSM-6510LV JEOL. In SEM, highly energetic and accelerated electron beam interact with sample and produce variety of emission are detected by sensors. Figure 3.2 shows the schematic diagram of working principle of the SEM microscope.

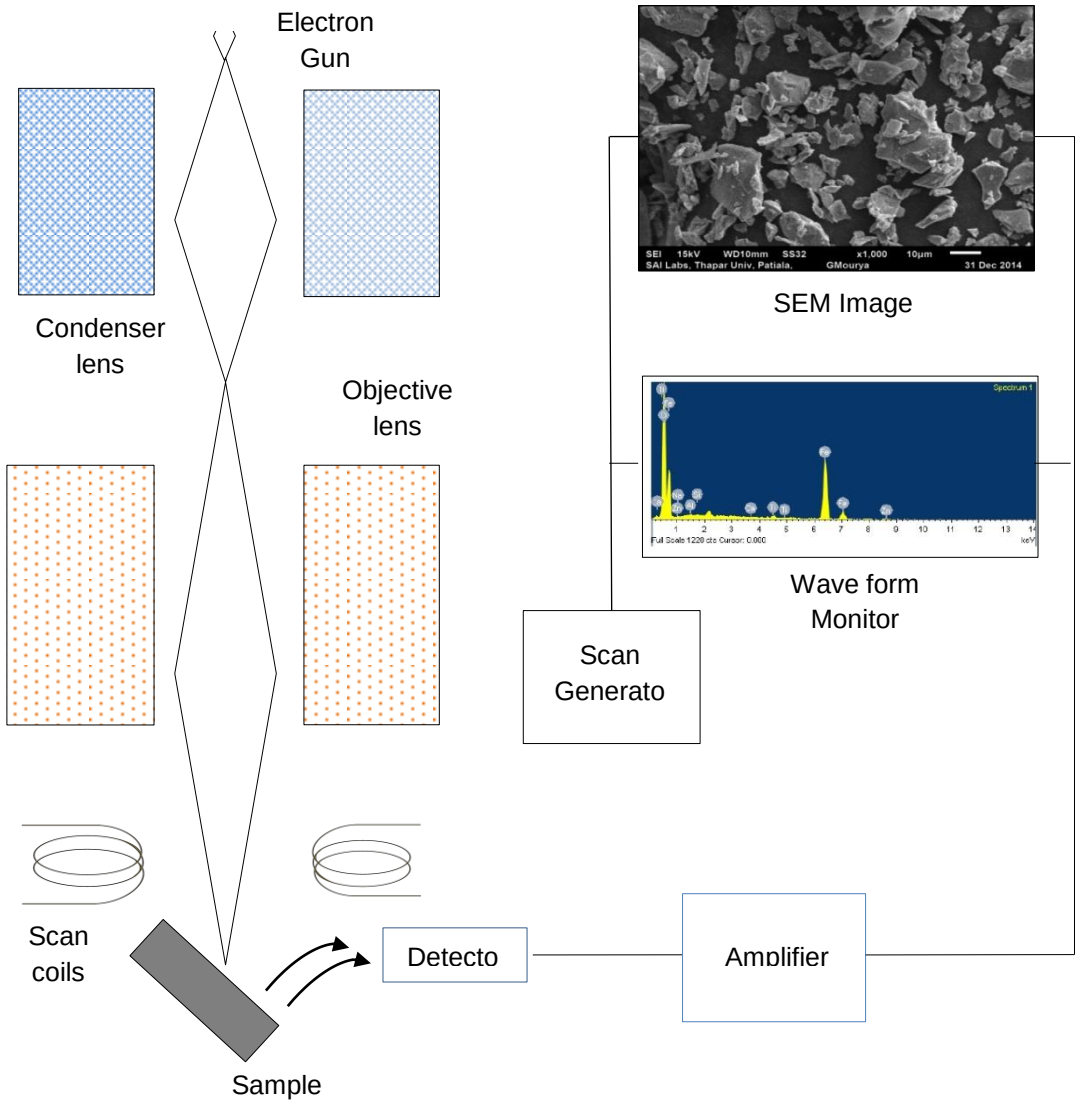

Figure 3.2 Working principle of scanning electron microscope (SEM)

The EDS analysis sensor is used to differentiate the energy spectrum and preinstalled EDS software is used to analyze and determine the elements. The EDS analysis gives the detail about the composition of material.

3.3 X- Ray diffraction Analysis (XRD)

A crystal lattice is defined as a systematic distribution of atoms in three dimension space. X-ray diffraction is used for the identification of phase and crystalline material and also provides the information about the unit cell. The working principle of X-ray diffraction is constructive interference of ray of single wavelength (i.e. monochromatic wavelength) with the crystal structure of the sample. The incident ray strikes with sample and generate constructive pattern of interference to satisfy the Bragg's law conditions. According to the Bragg's law (eqn. 3.1), the diffraction will occur when monochromatic beam of rays of wavelength λ incident at an angle (θ) on the lattice plane of the crystal structure. The law depicts the relation between the electromagnetic radiation and the angle of diffraction also with the lattice spacing of crystal structure of the sample to be tested.

$$m * \lambda = 2d * (\sin\theta) \tag{3.1}$$

Whereas, '*m*' is defined as the reflection order and is a positive integer.

Plotting the graph by changing the angular position and intensity of the rays is the resulting diffraction peak which characterizes the sample. When a mixture has different phases such as amorphous and crystalline, the diffractogram is obtained by the individual pattern of phases. The sharper peaks in diffractogram depict the finer crystalline structure of sample. The X-ray diffraction of sample were collected by Phillip X'Pert diffractometer (Model: PW 1710), at working voltage of 40 kV and 30 mA using Copper Kα radiation (λ=1.542Å) the sample scanned over a scattering angle 2θ from 0 ± 80^{O}. X-rays are direct on to the sample. Both the samples and the detectors were rotated and the intensity of the reflected X-rays was recorded. A detector collected and process the X-ray signal also converted that signal into the count rate which is further displayed on the output screen.

Figure 3.3 Phillip X'Pert X-ray diffractometer (Model: PW 1710)

3.4 Rheometer

Rheometer is a device used to study the flow behavior of the liquids and solid-liquid slurries. It usually deals to calculate approximate way of deformation under the effect of applied shear stress. There are several types of rheometer available to investigate the fluid behavior such as Newtonian/non-Newtonian, viscosity, shear stress, deformation rate, relaxation time and elongation viscosity etc. The cone plate concentric cylinder type Rheometer are widely used to determine the rheological characteristics of solid-liquid suspension (Al-Zahrani and Al-Fariss, 1998).

3.4.1 Types of rheometer

Concentric cylinder

In the concentric cylinder rheometer, there are two concentric cylinders is used. One cylinder is fixed and other is driven at constant torque motor. The viscosity of fluid measured between two concentric cylinders governs the rotation. The faster spin of rotation at given torque lower the viscosity is measured. The elastic modulus is calculated as function of shear stress. In order to measure the elasticity, viscoelasticity and viscosity of non-Newtonian liquid concentric cylinder rheometer is used.

Parallel plate

Parallel plate rheometer is used for those samples which is independent on shear rate. Parallel plate is not used for non-Newtonian fluid. In the parallel plate rheometer bottom plate is stationary and upper plate is rotary. A constant speed motor is installed on upper plate and a sensor is attached to determine the angular deflection or strain rate.

Cone and plate

The working cone and plate rheometer is quite similar to parallel plate rheometer but upper plate is replaced as cone. Cone has slight angle and constant shear strain throughout the sample. So it is used for non-Newtonian fluid. The components of concentric cylinder rand cone plate are shown in **Figure 3.4**.

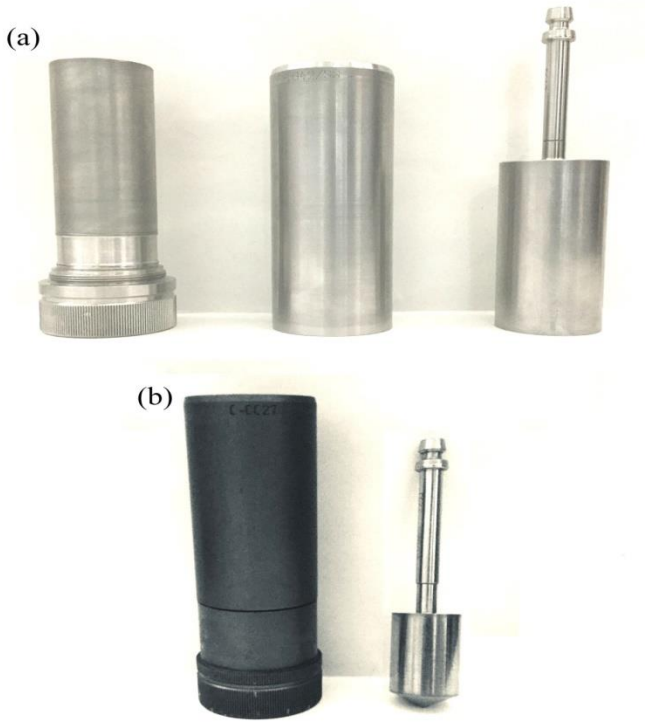

Figure 3.4 (a) Cylinder cup and rotating bob assembly (b) Cone and Cylinder rheometer assembly

Figure 3.5 Rheometer (Rhelolab QC Anton Paar) used for rheological experimentation

3.4.2 Working methodology of rheometer

A constant torque motor is connected to the Rheometer which works through the various arrangements of the Rheometer. A sensor which is used to measure the angular position or movement by the system is connected with the shaft. A constant speed motor and the torque detection system is installed with rheometer. An assembly of torsion bar is suspended in an air to provide hypothetical frictionless bearing. As a result of rotation of driving system, the sample offers resistance to the motion and tries to twist the torsion bar. As the stiffness of the bar is known by measuring the resultant twist with the help of angular position detector, the torque can be obtained.

The product of angular velocity and torque with the "form factors" C_1 and C_2 to find out the shear stress, τ and shear rate γ, respectively

Shear Stress $$\tau = C_1 \times M \quad (3.2)$$

Shear rate $$\gamma = C_2 \times \omega \quad (3.3)$$

Viscosity $$\eta = \tau \times \gamma \quad (3.4)$$

Whereas M denotes the torque and ω represents the angular velocity.

In some measuring systems the arrangements like parallel plates, the gap between the measuring systems is adjustable and can be set by the user. In this case the equation used is:

$$\gamma = \frac{C_2 \times \omega}{L} \quad (3.5)$$

Where, L denotes the gap.

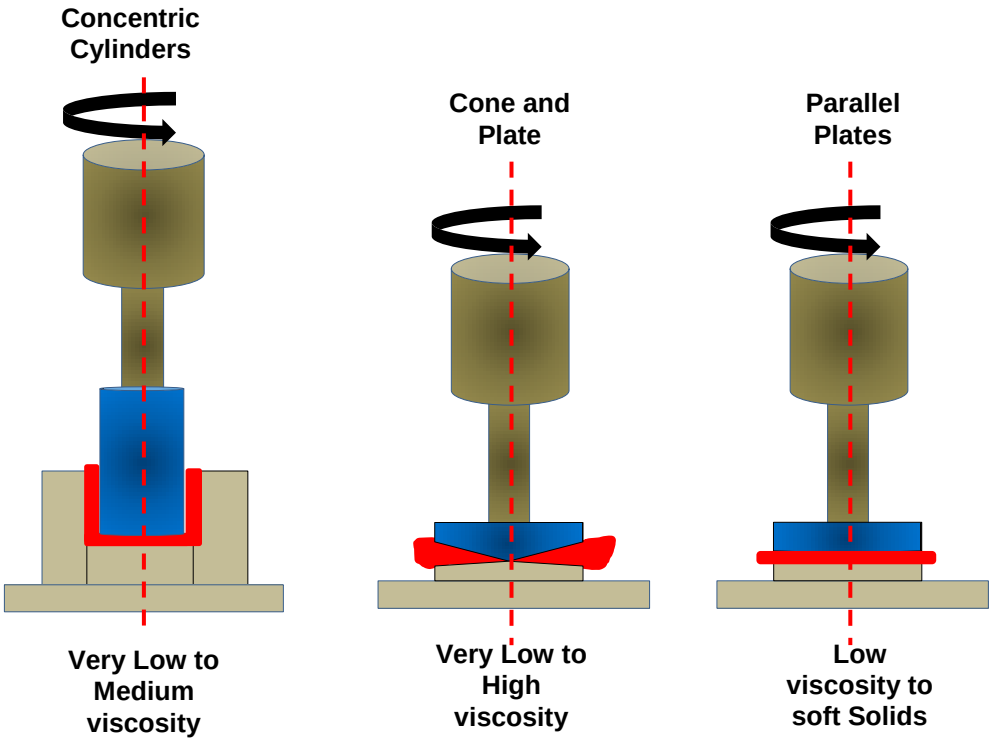

Figure 3.6 Different types of rheometer

Form factors are related to the various arrangements used with measuring systems and the equations are:

Cone plate: $C_1 = \frac{1}{\frac{2}{3}\pi r^3}$ and $C_2 = \frac{1}{\theta}$

Where 'r' represents the radius of cone, and 'θ' denotes the cone angle in radius

Parallel plates: $C_1 = \frac{1}{\frac{2}{3}\pi r^3}$ and $C_2 = \frac{3r}{4}$

Co-axial cylinders: $C_1 = \frac{1}{2\pi r^2 H}$ and $C_2 = \frac{2r_1^2 r_0^2}{r_a^2(r_0^2 - r_i^2)}$

Where $r_a = (r_i + r_0) / 2$

r_i represents the inner radius; r_0 denotes the outer radius

and H; is the height of cylinder

3.5 Preparation of slurry sample

To perform rheological tests, 50 ml of slurry samples of varying solid concentration of both fine and multivariate slurry sample. The slurry sample was prepared by mixing known weight of solid with water. An electronic type single pan balance with least count of ±0.001 mg was used to measure the weight of iron-ore sample. In order to ensure proper mixing of aqueous suspension of slurry a glass rod was used to stir the mixture for 10-15 minutes. The different Rheometer assemblies like concentric cylinders and cone-plate were used to perform the experiments. Rheological tests were commenced by changing the shear rate value from 0 - 600 s^{-1} by varying solid concentration and temperature. Further experiments were extended to study the effect of bi-modal on the rheology of fine and random sized slurry. Each experiment was performed twice for in order to ensure the precision of measured data.

- In sample S-1 the slurry is prepared by mixing iron-ore of particle size 53-75 µm. Also the the blending of particle size less than 53 µm was done in the slurry sample S-1 at solid concentration varying from 10 to 40 % by weight.

- Whereas in sample S-2 the multivariate slurry is prepared as per the particle size distribution of sample and blending of particle size less than 53µm, 53-75 µm and 75-106 µm at solid concentration varying from 10 to 40 % by weight.

Figure 3.7 Iron-ore and Iron-ore water slurry sample

Chapter 4

Physical and Chemical Characteristics

While designing a slurry transportation system at various industries such as mineral processing, thermal power plant and mine station, it is necessary to analyze the physico-chemical properties and mineral properties of solid material as well as slurry suspension. In this chapter, discussion is made on physico-chemical and mineralogical properties on the samples of iron-ore in following section.

4.1 Particle size distribution

Particle size distribution is method to calculate the diversity present in the size of the particles in a sample. The diversity in particle size of samples was analyzed with the help of standard mechanical sieve shaker. **Figure 4.1** and **Table 4.1** depict the detail about the percentage of finer present in range of particle size. The sample is sieved for 30 minutes through set of sieves of size 355, 250, 150, 106 and 53 µm. The weight of the particles retained on each sieve procured carefully, calculated and expressed in percentages. Samples were dried in oven at $105^{O}C$ for 30 minutes to ensure that there was no moisture in the sample. In S-1, about 54.6% particles were found to be less than 53 µm. Approximately 38, 5.0, 2.3 and 0.1% were lie in the range of 53-75, 75-106, 106-150,150-250 and 250-355 µm respectively. However in second sample S-2 nearly 28.2% particles have size less than 53 µm. Whereas 24.2, 42.5, 3.3 and 1.8% particles lie in the range of 53-75, 75-106, 106-150,150-250 and 250-355 µm respectively.

Table 4.1 Particle size distribution

Sieve size (micro-meter)	**Mesh Size (milli-meter)**	**Fraction (gm)**		**Commulative weight %(under)**		**Commulative weight %(Over)**	
		S-1	**S-2**	**S-1**	**S-2**	**S-1**	**S-2**
<53	0.053	54.6	28.2	54.6	28.2	45.4	71.8
53-75	0.075	38	24.2	92.6	52.4	7.4	47.6
75-106	0.106	5	42.5	97.6	94.9	2.4	5.1
106-150	0.15	2.3	3.3	99.9	98.2	0.1	1.8
150-250	0.25	0.1	1.8	100	100	0	0

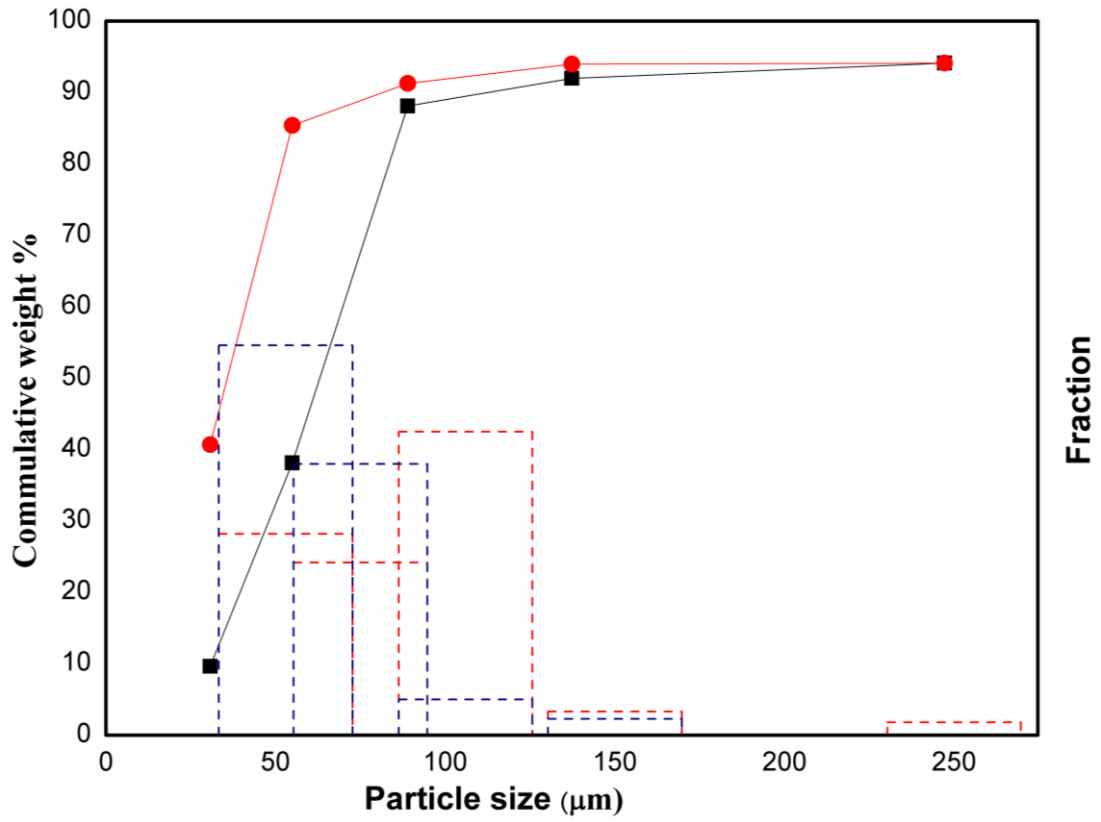

Figure 4.1 Particle size distribution of sample.

4.2 Maximum Settled concentration (C_w^{max})

Maximum settled concentration is measure of the maximum possible static concentration of suspension obtained while kept for specific time in range of 24-48 hours. C_w^{max} is a function of specific gravity of the material and the solid concentration of the suspension. It is important to study C_w^{max} value as for analysis and economical design of slurry pipeline. The maximum value of static settled concentration of iron-ore in slurry suspension was calculated by gravitational method. During transportation of iron-ore-water slurry, while the solid concentration approaches to maximum value of settled concentration specific energy consumption increases. The slurry of solid concentration ranging from 20-50% (by weight) was prepared and allowed to settle down in measuring cylinder for 24 hours after which there was no further settling of solid was observed. Maximum static settled concentration (C_w^{max}) was computed by relation as mentioned below.

$$C_w^{\max} = \frac{w_s}{w_l + w_s} \quad (4.1)$$

Whereas. w_s denotes the weight of solid in settled mass; w_l repersents weight of water in settled mass. The settling is very fast at initial stage i.e. 3-4 minutes afterwards reaches to static settlement level and difference in level of slurry in measuring tank is very minute after one hour time period. The value of C_w^{max} for 30%, 40%, 50% and 60% concentration of iron-ore-water suspension is tabulated in **Table 4.2** below

Table 4.2 Physical Properties of Slurry sample S-1 and S-2

Solid Concentration		Maximum Settled concentration (C_w^{max})	Potential of Hydrogen (pH)	Slurry density (Kg/m^3)
Slurry Sample S-1	30%	73.58	8.93	1250
	40%	77.93	8.97	1422
	50%	83.56	9.02	1555
	60%	87.2	9.08	1786
Slurry Sample S-2	30%	79.93	8.97	1320
	40%	85.49	9.02	1470
	50%	88.78	9.05	1661
	60%	93.8	9.08	1820

4.3 Potential of Hydrogen (pH)

The pH value of the iron-ore-water suspension was measured to describe its chemical nature whether acidic or alkaline. After calibration of digital pH meter with buffer solution, the pH was measured and found that slurry is alkaline in nature. The level of alkalinity increases with increase in solid concentration. The alkaline behavior of iron slurry can be explained due to fact that iron as being a reducing agent increases the amount of OH^- ions in the suspension. The pH value of slurry at different concentration is tabulated in Table. The value of pH at solid concentration of 30%, 40%, 50% and 60% of iron-ore water suspension is tabulated in **Table 4.2** above. The pH of slurry suspension was changes due to presence of alkaline layer and elements associated with the particles. As the solid concentration was increased the outer associated layer dissolves in water which results in increase acidic of

slurry suspension. So as the solid concentration was increases pH of slurry suspension was decreases.

Specific gravity is the measurement of density of material with respect to the standard material such as for gasses air is taken as standard material and for liquid water as standard material. Specific gravity of iron-ore water slurry was determined by following ASTMC 128. The specific gravity slurry suspension also influenced the static settled concentration. The specific gravity of slurry plays an important role in designing of slurry transportation system. In present work the pycnometer method was employed to calculate the specific gravity of samples.Samples were dried in oven for 30-45 minutes at temperature of 110^{O}C to ensure that the moisture is completely removed from the sample. A measuring cylinder of 200 ml was weighed before and after pouring known weight of samples. Water was added in to the flask up to fixed level in order to make desired concentration and then mixture was stirred for 15 minutes with help of glass rod. Lastly, the distilled water was poured up to same level and its weight was noted down. The specific gravity of fly and bottom ash samples were calculated by using following equations:

$$\text{Specific Gravity } (\sigma) = \frac{(W_{CS} - W_B)}{(W_{CW} - W_{CSW}) + (W_{CS} - W_B)} \tag{4.2}$$

Where W_C = Weight of measuring cylinder (gram), W_{CS} = Weight of flask and solid (gram), W_{CW} = Weight of flask with water (gram) and W_{CSW} = Weight of flask with solid and water (gram).

4.4 Scanning Electron Microscopy (SEM) and Energy Dispersive Spectroscopy (EDS)

SEM and EDS are commonly used to study the morphological characteristic and for the quantative analysis to determine the elements present in specimen. In SEM analysis greater resolution superficial images are produced because of narrow electron beam which result in a distinctive 3-D appearance which is beneficial in surface analysis of the sample. The scanning electron micrographs of sample S-1 and S-2 are shown in **Figure 4.2 (a)** and **Figure 4.2 (b)**. From figure it was noticed that the particle of iron-ore were crystalline fibers and granular in nature.

The white blister spots in the figure were may be due to the mine fire. The dark areas in the micrographs were mostly Fe_2O_3 whereas the bright portion of samples was Ti and Si. Titanium was observed in the results of chemical analysis as slag inclusion which might increase the the Titanium content in the samples.

The spectrum analysis in EDS gave the detail about the various elements present in the sample. The details of elemental composition of samples are tabulated in **Table 4.2**. In spectrum peaks were observed subsequent to the various elements of sample. In sample S-1 the weight percentage of Oxygen was noticed 23.03% and iron 74.5%. Other elements such as calcium (Ca), silicon (Si) and aluminium (Al) were present in small proportion. Similarly from the spectrum of sample S-2 it was observed that the weight percentage of iron was 68.2% and weight percentage of oxygen was found to be 25.8%. Also EDS analysis give details about the various compounds present in sample such as in sample S-1 the compound percentage of SiO_2, TiO_2, and FeO was found approximately 3.37%, 1.42% and 92.91% respectively. However in sample S-2 the compound percentage was found of SiO_2, TiO_2, and FeO approximately 19.40%, 1.43% and 78.97%.

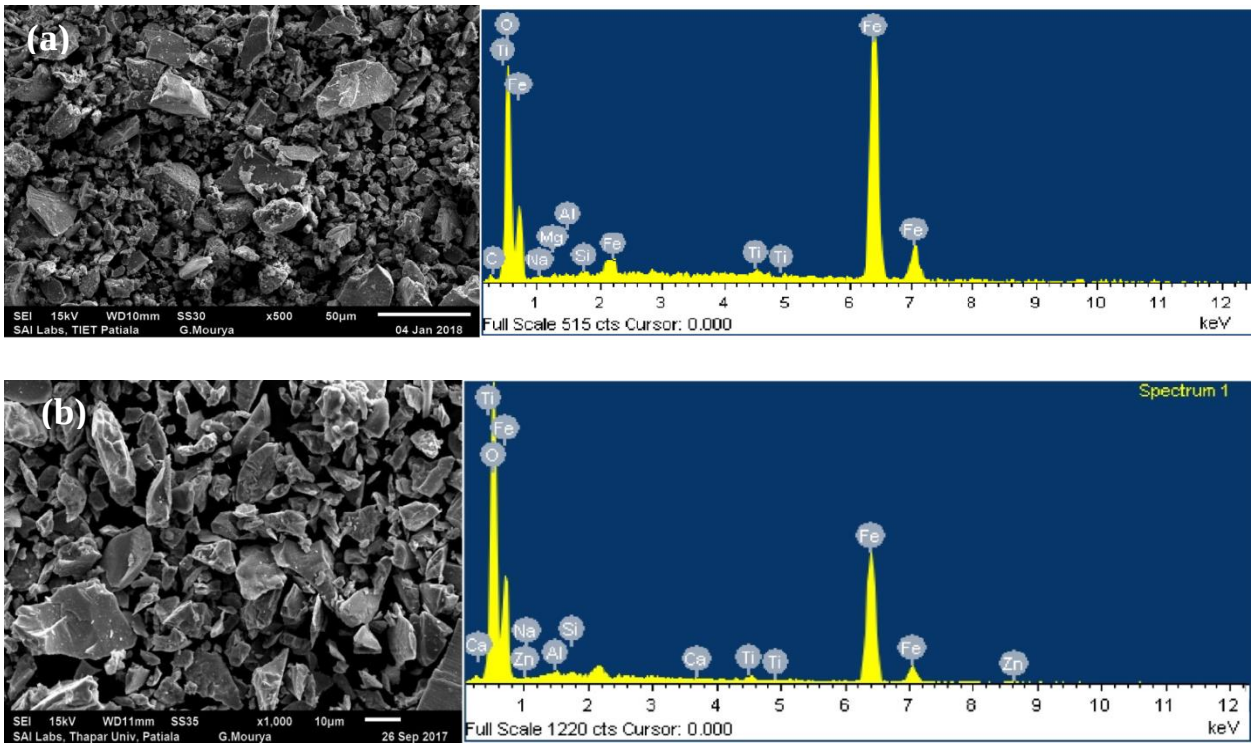

Figure 4.2 SEM and EDS analysis of sample S-1and S-2

Table 4.3 Elemental compositions of sample S-1 and S-2

Elements		Fe	Si	Ti	Ca	Al
Sample	S-1	74.55	1.12	0.37	0.21	0.72
	S-2	68.2	2.32	0.23	0.19	0.56

Table 4.4 Compounds detected in samples

Compounds		FeO	SiO_2	TiO_2	CaO	Al_2O_3
Sample	S-1	92.91	3.37	1.42	0.14	2.16
	S-2	84.97	10.40	2.47	0.78	1.88

4.5 X-Ray Diffraction (XRD)

The XRD analysis of samples S-1 and S-2 are shown in Figure 4.3 and 4.4. From the pattern obtained in the XRD graph, it can be seen that the samples of iron-ore mainly consist of quartz and calcite. The pattern in the XRD graph depicted that hematite reduced to the magnetite and result in isolation of specimen due to low magnetic separation whereas the lower peaks of calcite showed that the decomposition of $CaCO_3$ and kaolinite was disappeared. In sample of magnetite ore (i.e. S-2) the primary component was iron and quartz was additionally existed which mean both iron and quartz (SiO_2) were fine scattered together and was difficult to isolate. Diffraction pattern produced sharp and strong peaks of iron due to crystalline nature of magnetite in S-2. However, the strongest peak of hematite (Fe_2O_3) was in close proximity to $2\theta=33.1619°$ with d-spacing 2.69932 Å and the quartz (SiO_2) was noticed in close proximity to $2\theta = 26.8025°$ with d-spacing 3.32333 Å is found in sample S-I. Also, the strongest peak of magnetite (Fe_3O_4) was observed nearly at to $2\theta = 57.0443°$ with d-spacing of 1.61327 Å and the quartz (SiO_2) was found close proximity to $2\theta= 53.4906°$ with d-spacing 1.71166 Å is found in sample S-2.

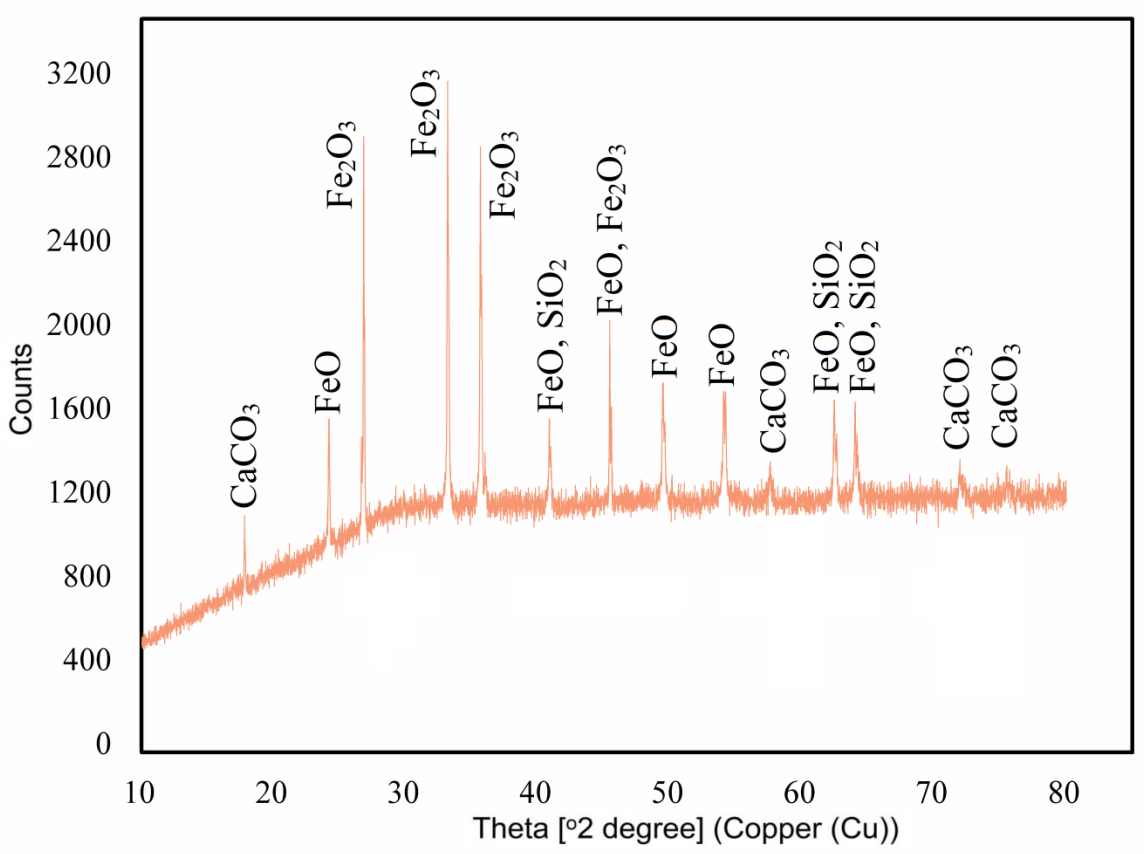

Figure 4.3 XRD analysis of sample S-1

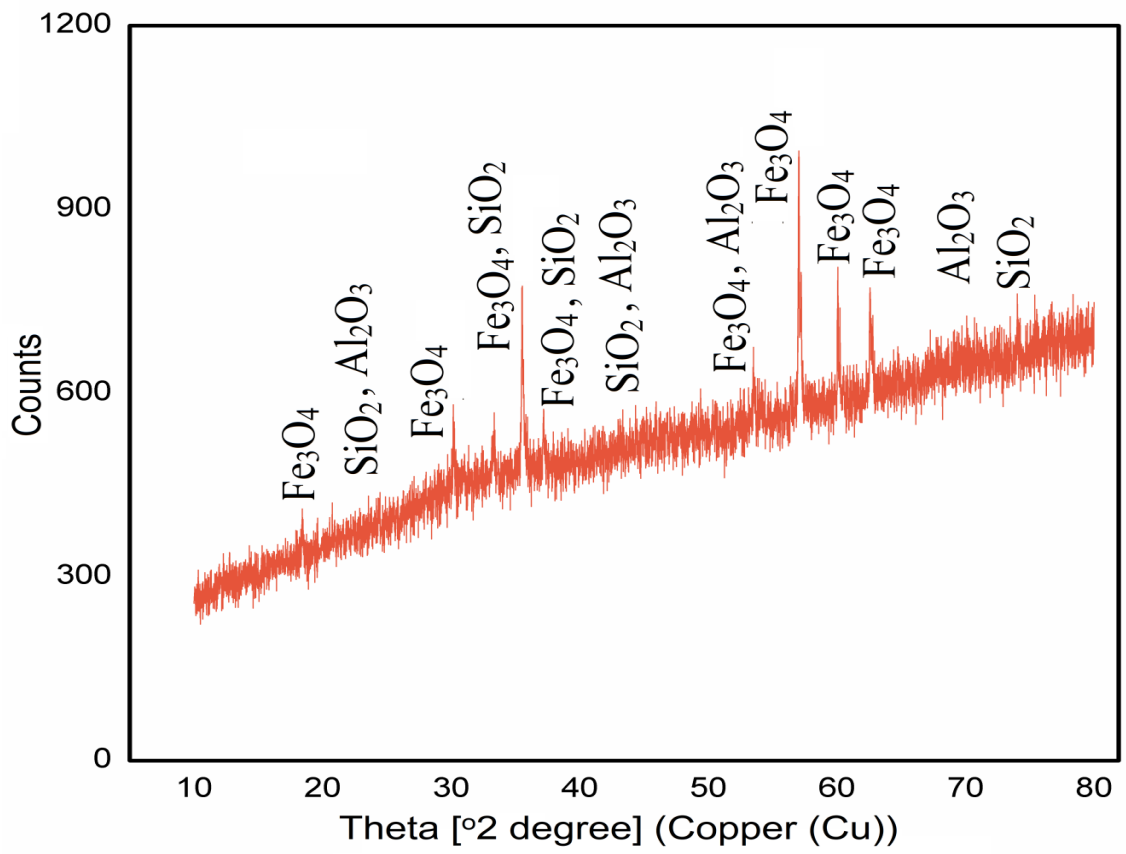

Figure 4.4 XRD analysis of sample S-2

4.6 Image processing

4.6.1 Prediction of shape factor

In present work, the SEM micrographs at magnification of 500× to 2000× were used to perform digital interpretation. Iso –threshold wad applied on SEM micrographs to determine the value of circularity factor of the sample particles presented in the **Figure 4.5**. During images processing analysis were performed on 5 dissimilarly shaped particles of iron-ore, sample of magnetite and hematite. From results, it is observed that the circularity factor for both the sample vary from 0.30 to 0.57 approximately whereas iron-ore particles confirms low circularity factor which indicated angular structure of the particles of iron-ore. The circularity factor directly affects the various processes such as head loss and fluid flow behavior etc.

4.6.2 Prediction of Solidity

An image analysis tool employs the pixel interpretation of roughness present in SEM image. By means of this, the grey value present in SEM image can be measured which is a calculative measure of average solidity of particles. The predicted value of solidity factor for samples of hematite and magnetite ore particles is represented in **Table 4.4**. From **Table 4.4**, it can be said that the solidity of both samples of iron-ore particles lies in a narrow range i.e. near to 0.99. The predicted values of solidity in present study hold good agreement with Liu *et al.*, 2017.

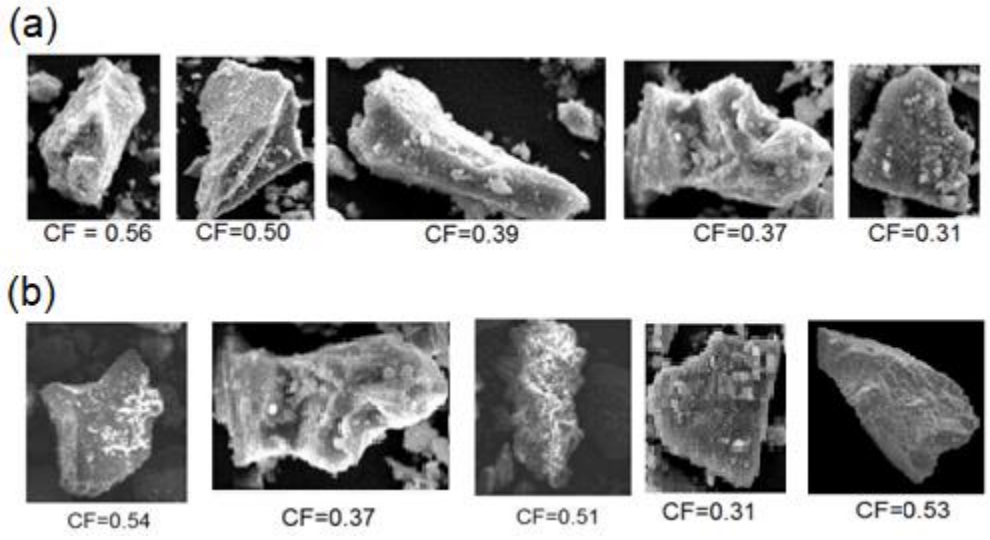

Figure 4.5 Circularity of (a) sample S-1 and (b) sample S-2 of iron-ore.

Table 4.5 Predicted ranges of shape parameters of various particles

Particle type	Circularity	Solidity	Sphericity
Hematite iron-ore	0.31-0.55	0.94-0.96	0.34-0.51
Iron-ore	0.30-0.56	0.96-0.98	0.36-0.54

4.6.3 Prediction of sphericity

Sphericity of particles of iron-ore samples are tabulated in **Table 4.4**. Image processing tool follows the correlation given by Zou and Yu (2015):

$$\varphi = \frac{As}{Ap} \tag{4.2}$$

Above indicates that sphericity is the ratio of sphere area to particle area which is measured from perimeter of random particles. The value of sphericity factor for both the samples of iron-ore was predicted in range 0.34-0.54 respectively. The tool is used to predict the value of sphericity on five different images of iron-ore sample.

4.6.4 Analysis of surface smoothness

The surface smooth of solid particles was analyzed using grey value interpretation of SEM micrograph. The SEM micrographs used for smoothness analysis are represented by Figure 4.6. In Figure, it can be seen that the surface profile of both samples of iron-ore particles forms large peaks (crust) and depth. Moreover, it exhibits non-uniform curve nature with high irregularities. The non-uniform curve nature for the sample of hematite and magnetite iron-ore with very frequent numbers of ups and down in figure clears the irregular surface of iron-ore sample.

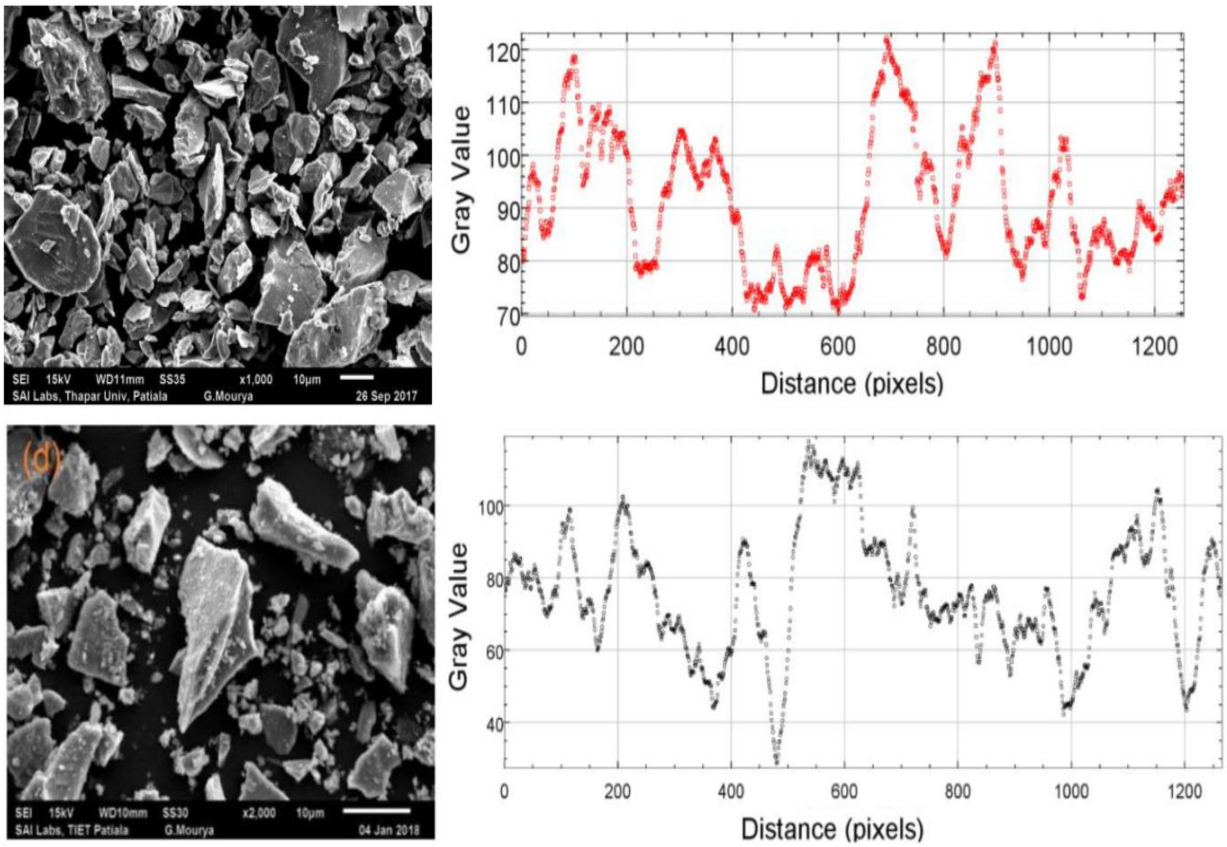

Figure 4.6 Surface smoothness of (a) sample S-1 and (b) sample S-2 of iron-ore .

Chapter 5

Rheological Characteristics

The mixture of solid and liquid is known as slurry, slurry generally undergoes a plastic deformation under the influence of external force or stress. The investigation of rheological characteristics of slurry suspension has been focused from many years due to wide applications in industries. Due to presence of solid particles, the study of flow characteristics of slurry suspension becomes a complex phenomenon. The physical properties of solid particles also affect the flow behaviour of slurry suspension. The change in flow characteristics of slurry may arises due to the application of shear stress and also due to the dissipation of external energy. The flow characteristics of slurry suspension depend on various factors like volume fraction, viscosity of slurry and the solid physical properties. The increase in solid concentration of slurry suspension shifts the flow behaviour from Newtonian to non-Newtonian and also results increase in viscosity of the suspension. Now-a-days the transportation of solid in the form slurry is mostly practices in many industries such as transportation of ore from mining industries and transportation of coal, ash from thermal power plant etc. However, the transportation of slurry suspension at higher concentration requires through knowledge of rheological behaviour of solid suspension at different solid concentration and flow condition. According literature survey, there are various parameters which plays crucial role to determine the rheological behaviour of solid suspension like viscosity, particles size, solid concentration etc.

5.1 Rheological characteristics of iron-ore-water slurry

The rheological experiments were performed to investigate the flow characteristics of multivariate slurry and the slurry prepared by fine particles of iron-ore. As sample S-1 consist of slurry prepared by fine particles whereas sample S-2 is slurry prepared by random sample procured. The rheological experiments were performed at different solid concentrations varying from 30-60% (by weight) for sample S-1 and solid concentration of 20-60% (by weight) for sample S-2. The shear rate is varied from 0-600 s^{-1} to measure the apparent viscosity of slurry suspension. The variation of shear stress with shear for sample S-1 and sample S-2 are shown in **Figure 5.1** and **Figure 5.2** respectively. From rheograms of iron-water suspension, it can be said that the flow behavior of iron-water suspension was highly influenced by variation solid concentration. From Figure 5.1, it was observed that the

shear stress is varying linearly w.r.t shear rate at 30% concentration. Further increase in solid concentration above 30%, the flow characteristics of slurry shifted toward the non-Newtonian flow behaviour. From experiment it was observed that slurry exhibits Pseudoplastic flow behaviour for solid concentration varying from 40 to 60%. Rheology results depict that shear stress is also a function shear rate. Initially high shear stress is required to initiate the shearing as initially more number of particles was at rest which means high inertia and required more force.

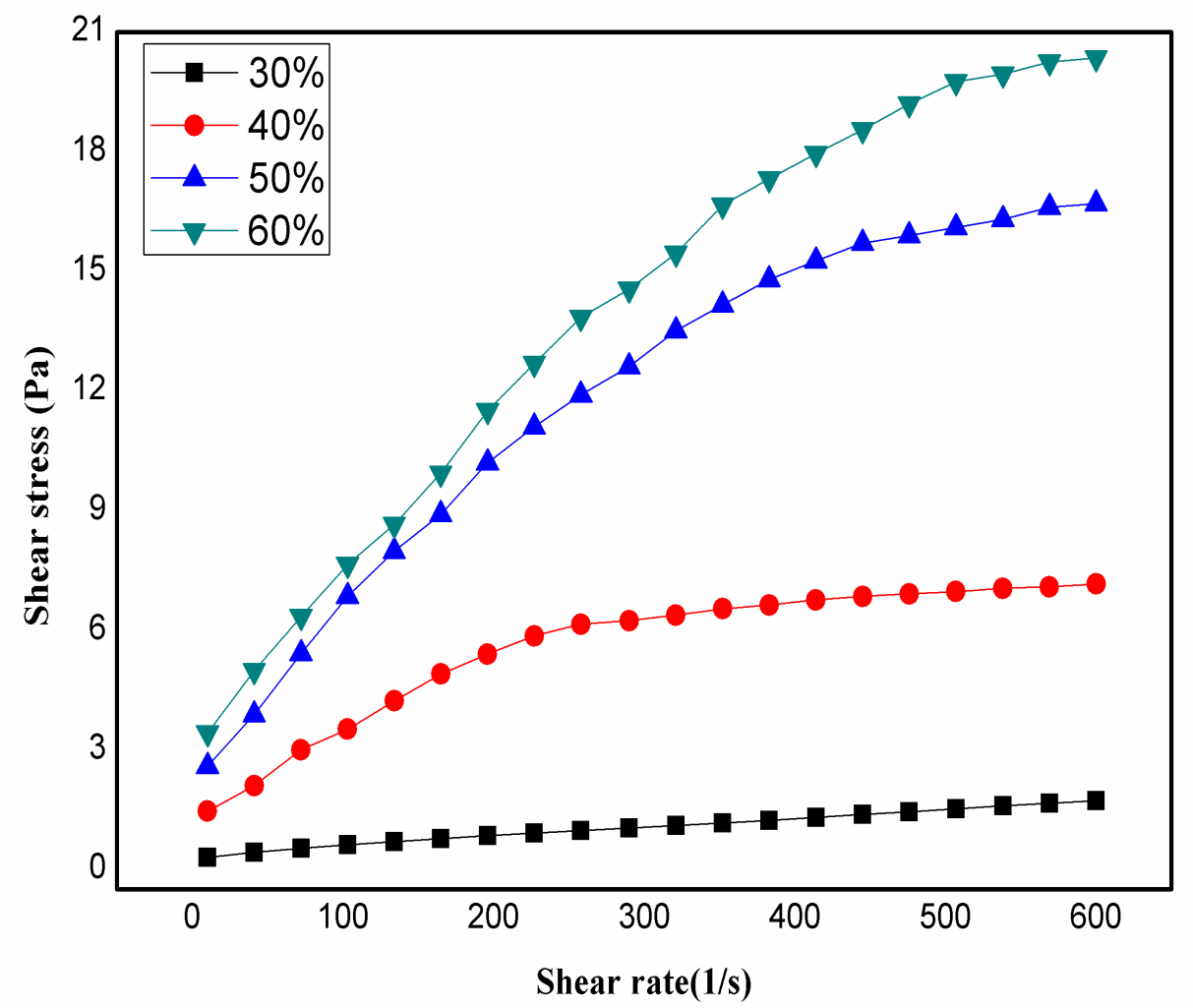

Figure 5.1 Rheograms of sampleS-1 at different concentrations

Similarly, the data obtained from rheology of multivariate iron-ore slurry is shown in **Figure 5.2**. From results it was observed that the flow characteristics of slurry were highly influenced by solid concentration and size of particles. As slurry in sample S-2 is prepared by

the random sample which contains particles according to the PSD of sample S-2 such as both fine and coarse particles are present in slurry. From result data it was observed that shear stress increasing steadily at lower shear rate whereas at high shear rate a rapid increase in shear stress was noticed. The reason for uneven slurry behaviour is due to the presence of particles of bigger size has, which means bigger particles have more inertia and required more force results steady increase in viscosity at high shear rate. The slurry behaviour at 30% concentration was noticed Pseudoplastic. Similar behaviour of slurry flow characteristics was also observed by many researchers (He, Wang and Forssberg, 2004; Chandel, Seshadri and Singh, 2009; Zhou *et al.*, 2010; Deosarkar and Sathe, 2012; Bobicki *et al.*, 2013) with different solid –liquid suspension including iron-ore.

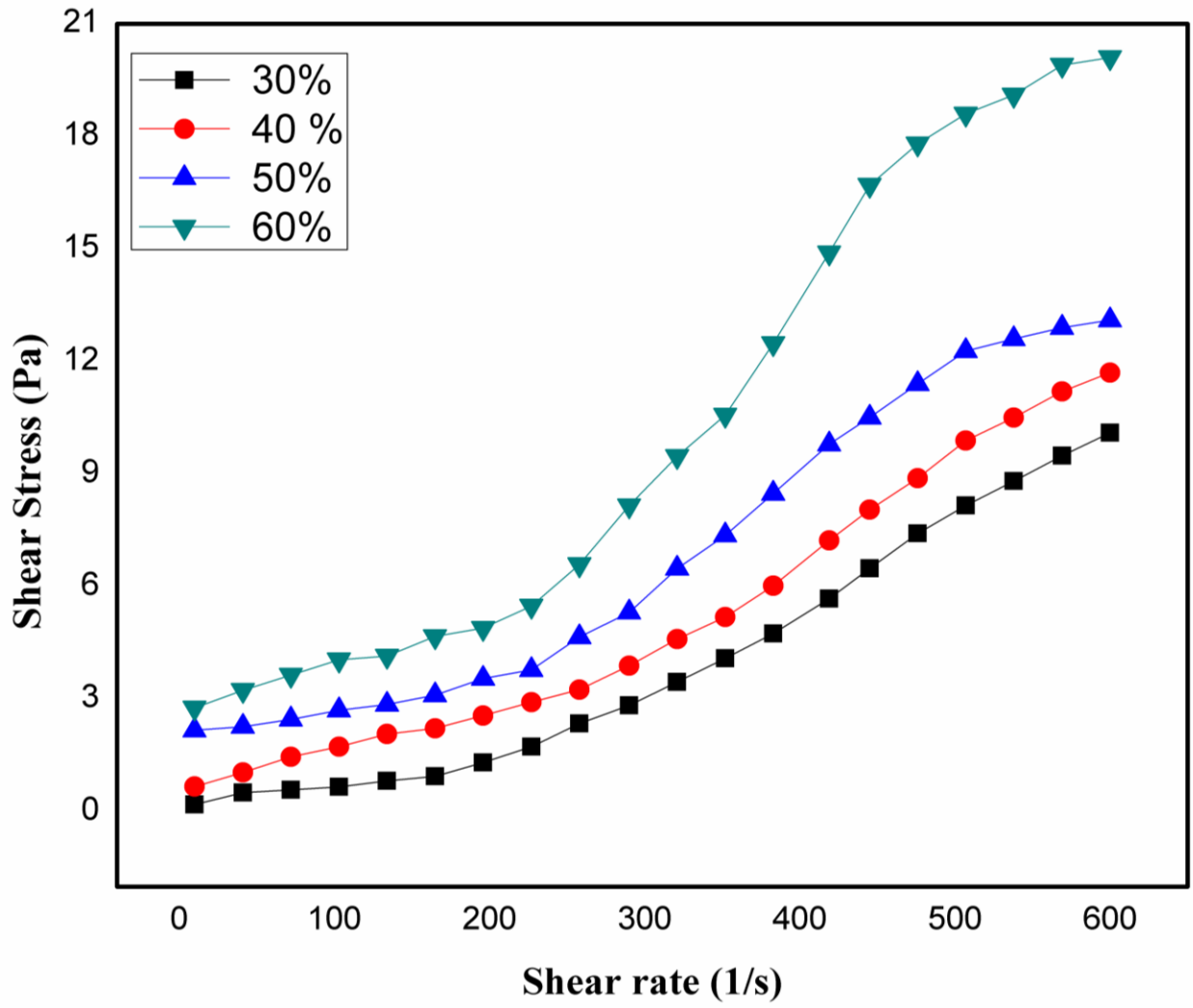

Figure 5.2 Rheograms of sample S-2 at different concentrations

5.2 Effect of solid concentration on apparent viscosity of slurry

As the solid concentration in slurry increases, the viscosity of suspension also increases. The increase in the slurry viscosity can be due to the increase in particle density in the slurry which results in increase in particle to particle interaction. **Figure 5.3** shows the variation of apparent viscosity with shear rate as well as sold concentration of sample S-1. From figure it can be seen that the apparent viscosity of slurry is a function of velocity gradient and solid concentration. From results it was observed that as the concentration of iron-ore in slurry increases the apparent viscosity of slurry also increases. The fact of increase in slurry viscosity with concentration can be attributed to the fact that as particle density increase lead to decrease in distance between the solid particles which results to decrease in amount of water trapped between the solid particles hence their mobilization decreases. However, similar results in increase in resistance to flow of ore-water slurry reported by Deosarkar and Sathe, 2012; Singh *et al.*, 2016. Similarly, initially high force is required to overcome the inertial resistance of particles which results in high apparent viscosity at low shear rate then viscosity decreases with shear rate and become almost constant.

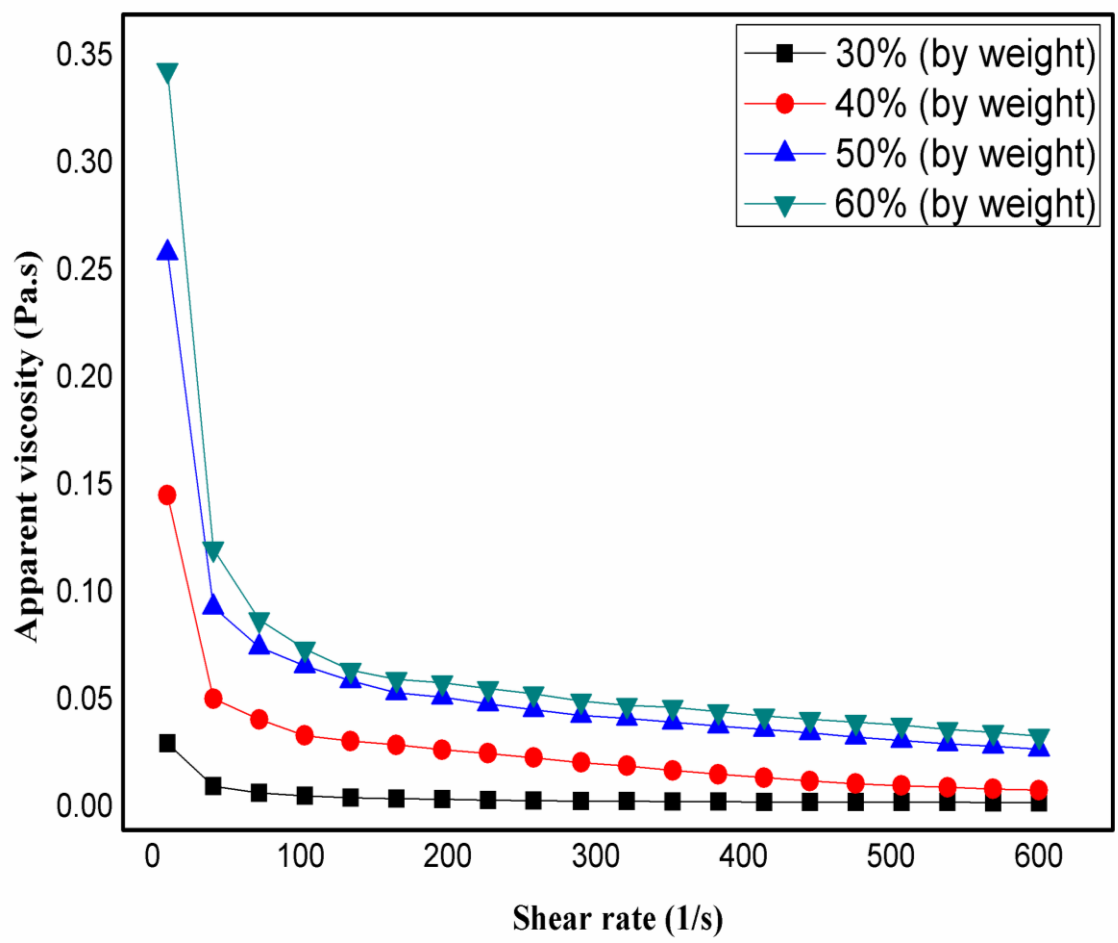

Figure 5.3 Variation of apparent viscosity with shear rate at different solid concentration of sample S-1

Similarly, the data obtained from the rheology experiment of sample S-2 is shown in **Figure 5.4**. Figure shows that the apparent viscosity of slurry increases with solid concentration. The fact decrease in apparent viscosity of the mixture attributed to the initially high force is required to accerlate the particles. The "pseudoplastic" or shear thinning behaviour of the slurry was noticed and the flow behavior of the slurry is almost Newtonian with slight degree of shear thinning up to the 30% concentration of the slurry and at higher solid concentration the pseudoplastic behaviour of the slurry become more predominant. It can be attributed to the fact that at higher solid concentration viscous forces become more dominant and cause a breakdown of the slurry structure which results decrease in the slurry viscosity with an increasing shear rate. At higher shear rates, the slurry structure is highly influenced by viscous forces and results distortion of the slurry structure to become, hence shear thinning behaviour of slurry was observed. Also, the increase in solid loading leads to increase in the apparent viscosity and shear stress of mineral slurry as the inter particle interaction among the minerals particulates highly increases and the effective area under shear also increases.

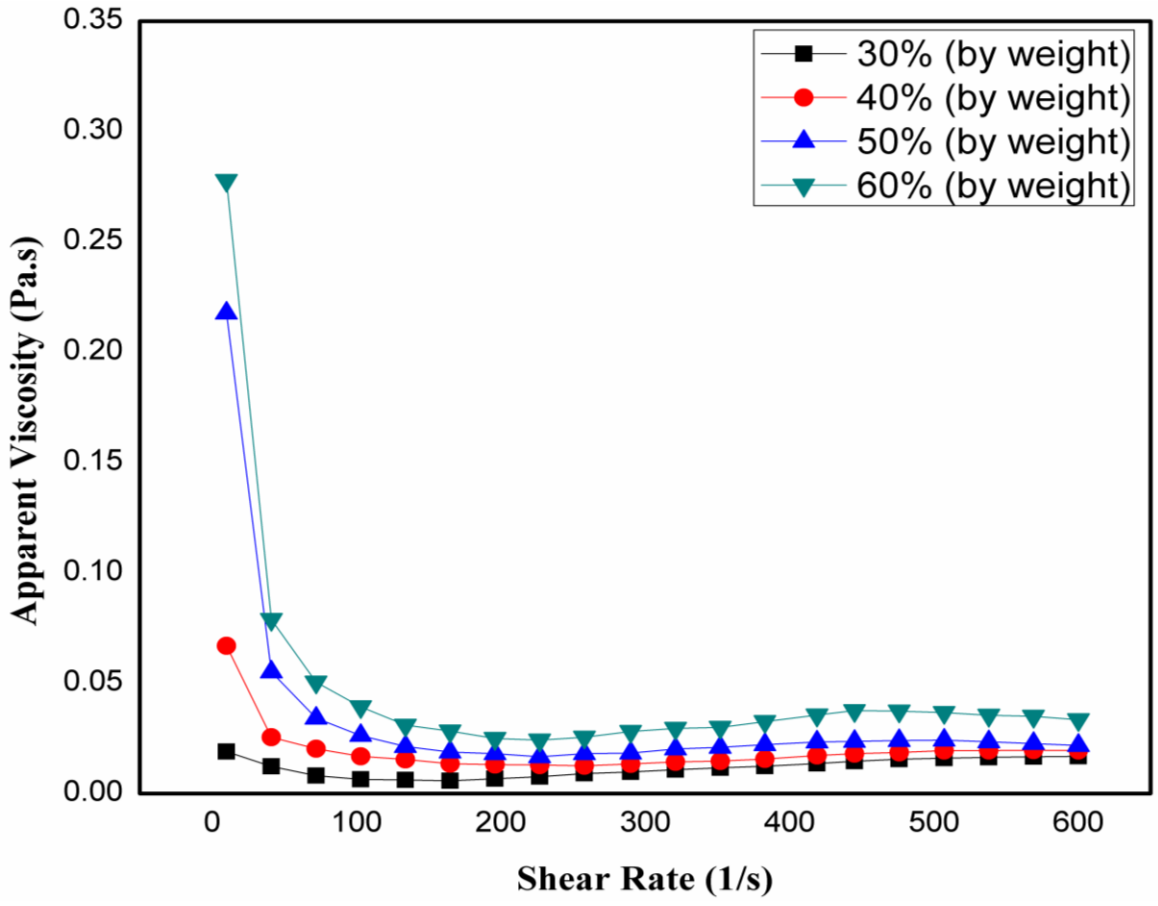

Figure 5.4 Variation of apparent viscosity with shear rate at different solid concentration of sample S-2

5.3 Effect of temperature on rheological characteristics slurry

The rheological experiments were extended to investigate the flow characteristics of slurry at varied temperature viz. 20±1.0ºC, 30±1.0ºC, 40±1.0ºC, 50±1.0ºC and 60±1.0ºC.for samples of slurry prepared by finer particles and the slurry prepared multivariate particles at solid concentration of 60% (by weight). The results obtained from the rheology experiments are presented in Figure 5.4 and Figure 5.5 for samples S-1 and S-2 respectively. From figures similar results were noticed in terms of variation with temperatures for both the slurry samples prepared by multivariate and finer particles of iron-ore. The reduction in the viscosity of slurry is in agreement with the mechanisms of momentum transmission in gasses or liquid due to elemental impact which means that the resistance offered by the carrier fluid decreases with increase in temperature. In other words, the rise in temperature results increase in kinetic energy of the iron-ore particles and also decreases the cohesive forces between the liquid molecules.

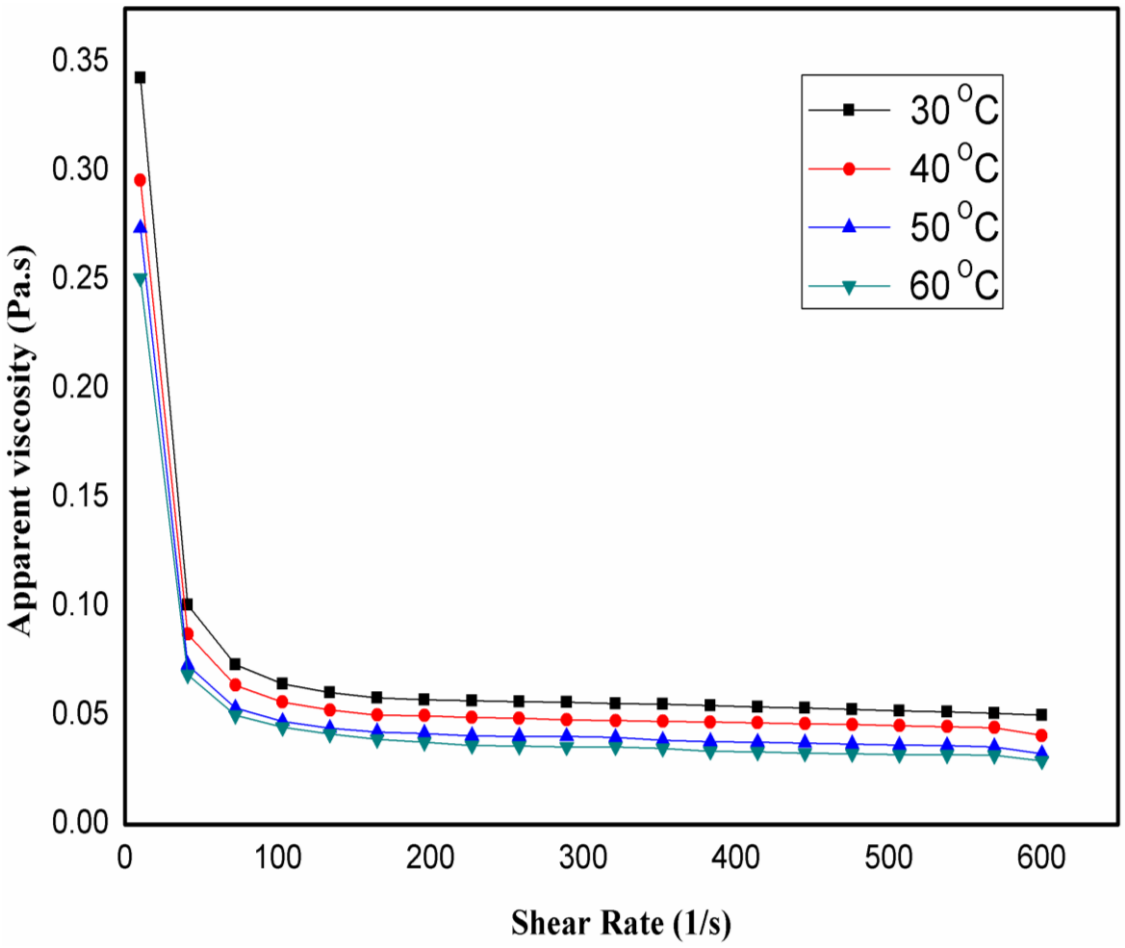

Figure 5.5 Effect of temperature on apparent viscosity of sample S-1 at solid concentration of 60% (by weight)

The relative viscosity of slurry dereases as the temprature increases which repersent the basic property of any viscous material. The increase in slurry temprature results in increase in kinetic energy of the carrier fluid particles of slurry, promotes to reduction in intermolecular forces between the adjacent layers of the fluid hence viscosity of slurry decreases with temprature. When slurry temperature increases from 30ºC to 40ºC, relative viscosity get reduced 13.66% and similarly when the slurry temperature rises from 40 to 50 and 50 to 60 ºC at solid concentration 60% by weight the relative decrease in viscosity is found to be 15.19% and 17.23%.

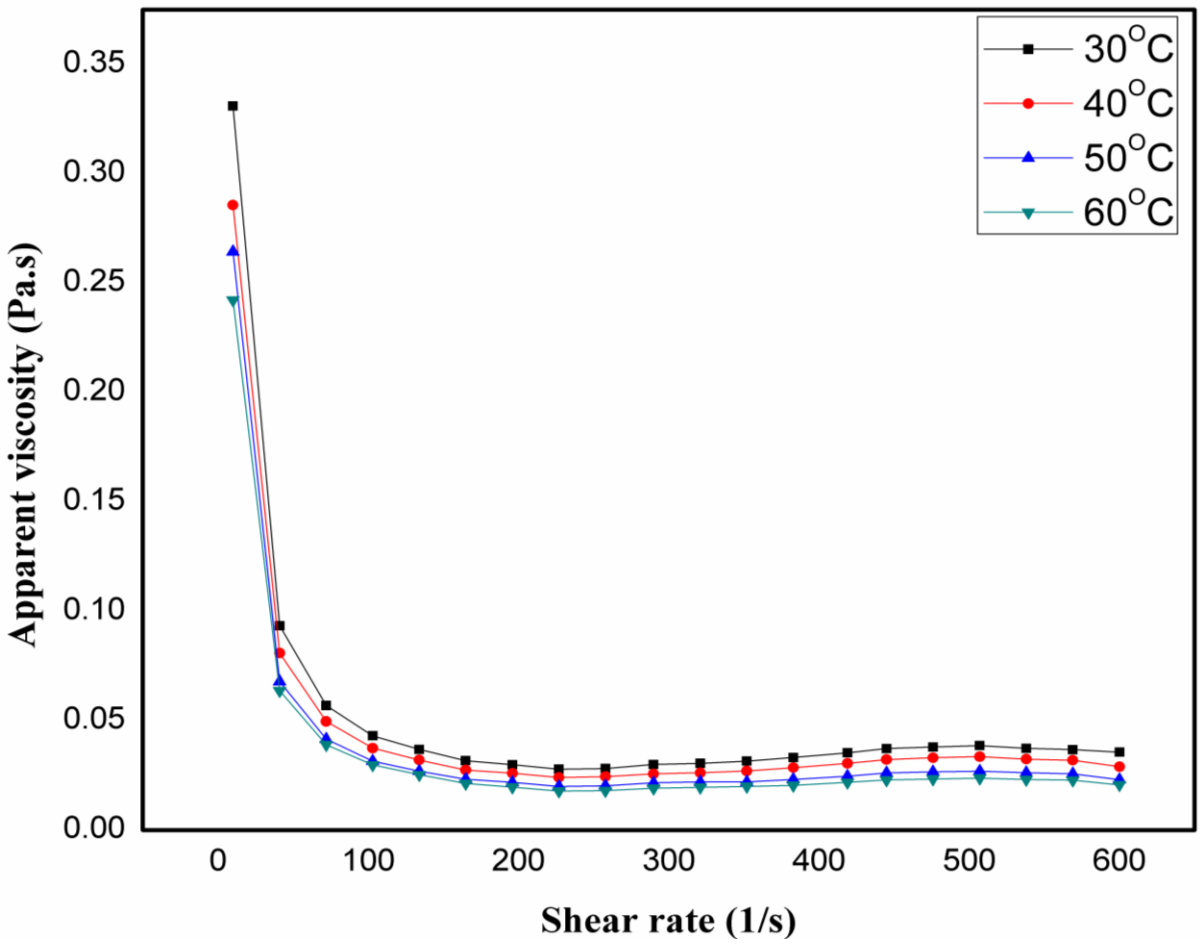

Figure 5.6 Effect of temperature on apparent viscosity of sample S2 at solid concentration of 60% (by weight)

5.4 Fitting into the rheological properties

Rheological models give information about the behavior of fluids by determining the nominal functions to develop a relationship between deformation rate and shear stress. Various empirical models were used to estimate the behavior of slurry is Power-Law, Herschel-Bulkley and Casson suspension:

$$\tau = k\gamma^{n} \tag{5.1}$$

$$\tau = \tau_{y,h} + k\gamma^{n} \tag{5.2}$$

$$\tau = \tau_{y,c}^{1/2} + (\eta_s \gamma)^{1/2} \tag{5.3}$$

where, k and n denotes the parameters of model known as flow behaviour index and consistency index respectively, and τ_y represents the yield stress. The shapes of the curves in depict that suspension exhibit the shear thinning behaviour at high shear rate. The pseudoplastic flow characteristic of an aqueous suspension of iron-ore in sample S-1 and S-2 can be described by Power-Law and Herschel-Bulkley model. In **Figure 5.7** and **Figure 5.8** the regression analysis is carried out to fit a particular model on experimental data associated with rheology. The correlation coefficient for model Herschel-Bulkley lies in range as follows; $0.95 < R^2 < 0.99$. In **Table 5.1** the model parameters of the rheological curves were tabulated. Yang and Aldrich (2005) performed experiments on magnetite-water slurry and found that flow characteristics could be described by Herschel-Bulkley.

Table 5.1 Parameters of rheological model

Solid concentration (by weight)		n	Type of flow
Sample S-1	30%	0.99	Newtonian
	40%	0.37	Pseudoplastic
	50%	0.504	Pseudoplastic
	60%	0.58	Pseudoplastic
Sample S-2	20%	1.8	Pseudoplastic
	30%	1.38	Pseudoplastic
	40%	1.32	Pseudoplastic
	50%	1.34	Pseudoplastic
	60%	1.63	Pseudoplastic

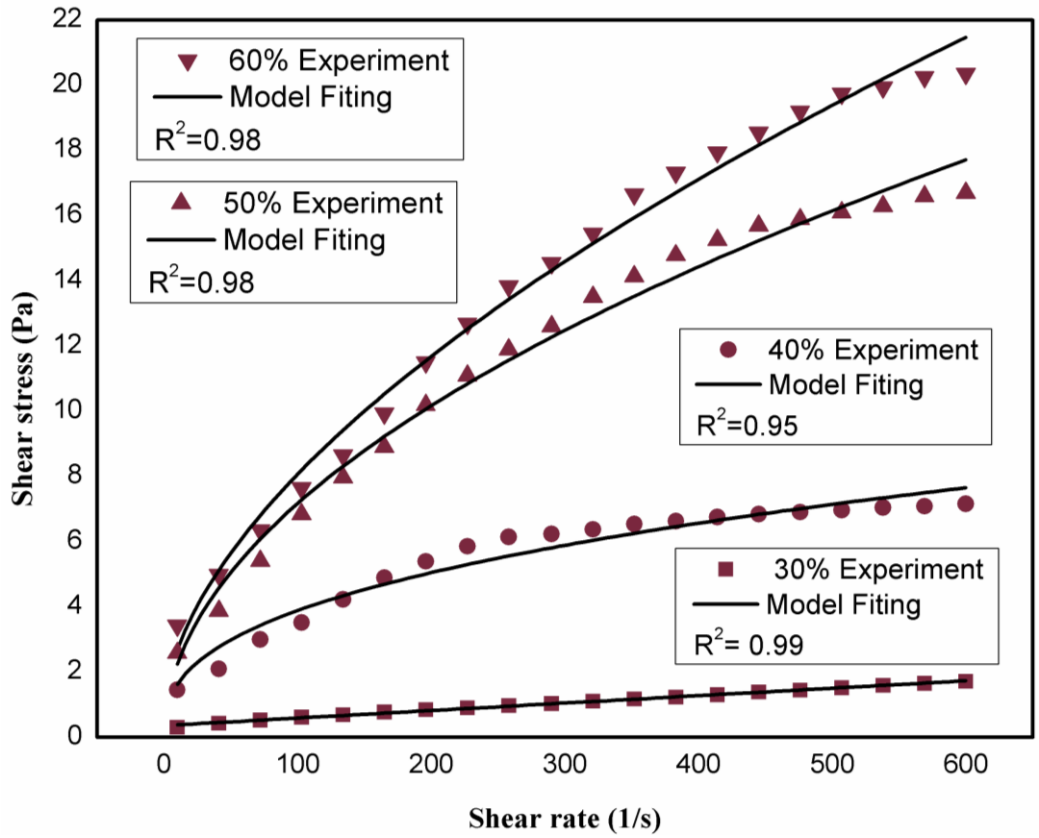

Figure 5.7 Rheological model fitting on experimental data at different solid concentration for sample S-1

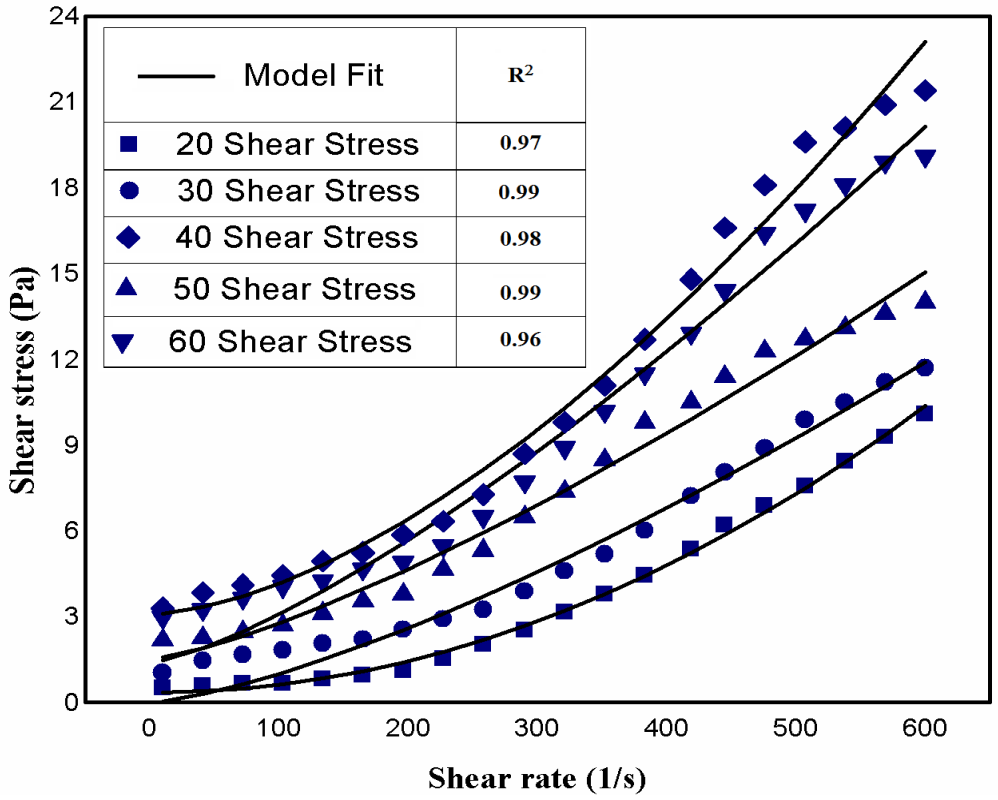

Figure 5.8 Rheological model fitting on experimental data at different solid concentration for sample S-2

5.5 Efect of bi-modal particle size distribution on rheology of iron-ore slurry.

The study was also focused on conveying of iron-ore-water slurry at maximum solid concentrations having low viscosity and at minimum transportation cost. So the series of experiments were performed by blending fine particles in coarser slurry suspension to determine flow characteristics of iron-ore water slurry. In case of soft solids like coal and coal ash surface irregularities decreased with increase in particle size which leads to decrease in apparent viscosity for coarser particle sized slurry. However, for hard solids like iron-ore surface irregularities increases with particle size which further results increase in viscosity of coarser particulate slurry as compared to fine particulate slurry (Ghanta and Purohit, 2002).

In sample S-1 the bimodal-slurry suspension of iron-ore was prepared by mixing finer particles i.e. <53μm within the slurry of 53-75μm whereas in case samples S-2 the bimodal slurry sample was prepared by mixing particles of <53μm, 53-75μm and 75-106μm with in the slurry of multivariate particle size. In order to determine optimum ratio of blending of finer particles in 60% concentrated solid suspension of 53-75μm sized and multivariate particle sized iron-ore-water slurry, the percentage of finer addition was varied from 10-40%. From experimental outcomes, it was observed that iron-ore-water slurry exhibits pseudoplastic behaviour as in the case of unimodal suspension. It was found that apparent viscosity of slurry decreases as the percentage of finer particles increases from 10-30%. The maximum decrease in viscosity was noticed by blending of 30% finer particles. The decrease in apparent viscosity may be attributed to fact that addition of finer particles (<53μm) in the slurry suspension increases particle dispersion and permits reduction of surface tension as well as inter-particulate forces (Singh et al., 2016). The relative percentage decrease in apparent viscosity with blending of 10%, 20% and 30% finer particles in coarser particles found to be 30.5%, 15.78% and 17.89% respectively at shear rate of 165 (1/s) whereas at shear rate of 600 (1/s) as shown in **Figure 5.9** for slurry prepared by sample S-1 and relative decrease in apparent viscosity was found to be 2.65%, 13.03% and 25.20%. Further increase in blending of finer particles to coarser suspension tends to relative increase in apparent viscosity as shown in **Figure 5.9**. The trend for bimodal rheological behaviour for coal water slurry was reported by Nguyen, Logos and Semmler (1997) and De Lorenzi and Bevilacqua (2002). The reducing trend in apparent viscosity supports to minimize the energy consumption and pressure drop during the flow of slurry suspension in the pipeline.

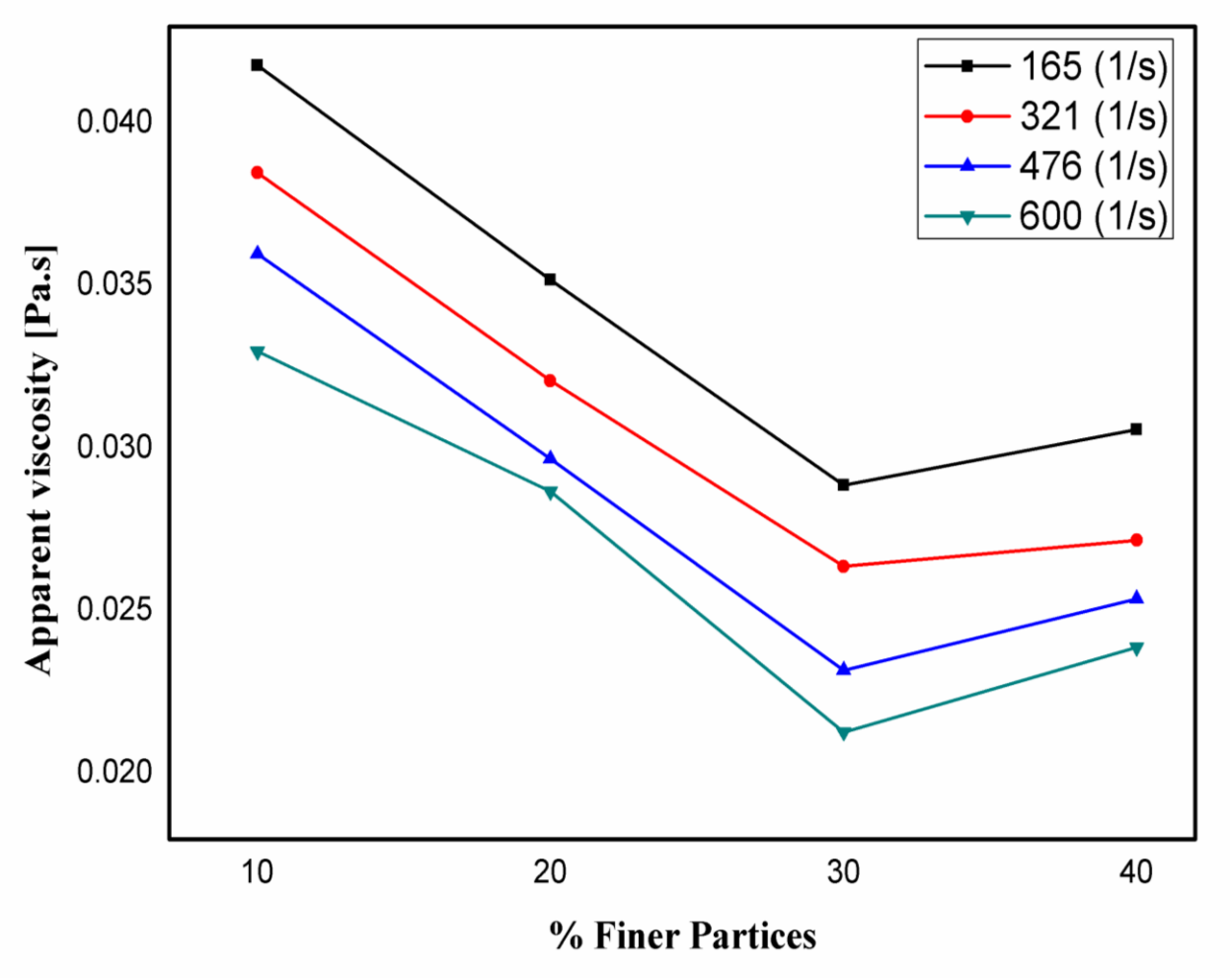

Figure 5.9 Effect of bimodal particle size distribution of size less than 53 μm on slurry of sample S-1

However in case of multivariate particulate slurry the blending of particulate of less 53 μm, 53-75 μm and 75-106 μm at blending concentration of 10%, 20%, 30% and 40% was done in order to determine the optimum blending ratio for each particle size. The relative decrease in apparent viscosity with the addition of particles of size less than 53 μm at blending concentration of 10%, 20% and 30% was found to be 29.32%, 18.96% and 17.19% for slurry prepared by sample S-2. The 20% blending is found to be an optimum solid concentration for the particulate of sized less than 53 μm, 53-75 μm and 75-106 μm. However, further increase in blending of finer particles to coarser suspension tends to relative increase in apparent viscosity as shown in **Figure 5.12**.

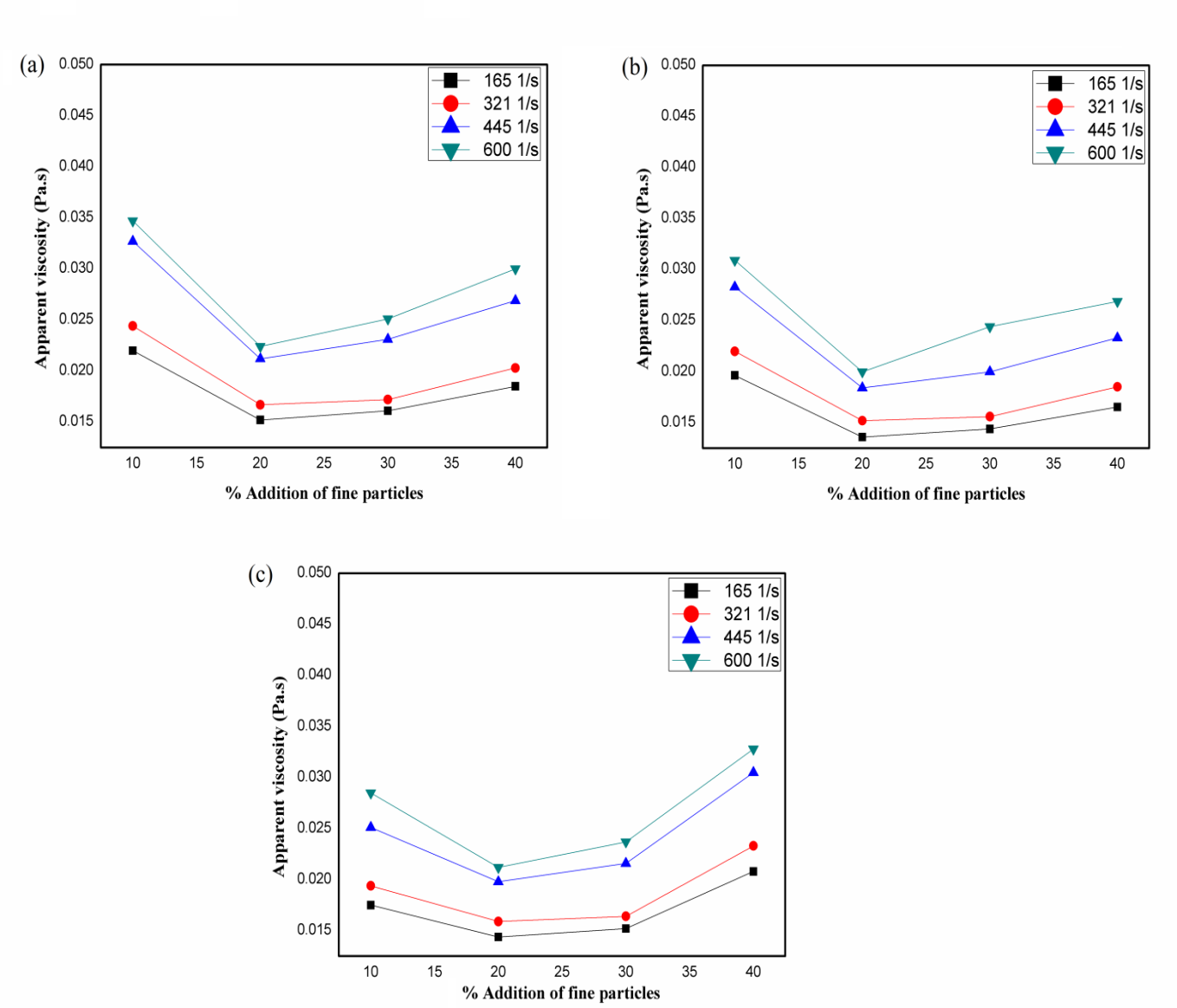

Figure 5.10 Apparent viscosity of sample S-2 with blending of iron-ore particle having size (a) less than 53 µm (b) 53-75 µm (c) 75-106 µm.

5.6 Prediction of apparent viscosity using Artificial Neural Network (ANN)

Neural networks are the prediction systems which provide the learning based knowledge about a process or approach [20]. In present investigation, MATLAB 16.0 was used to apply the neural network model namely standard multilayer feed-forward network. **Figure 11** shows three-layer neural network which consist of an input, output and hidden layer.

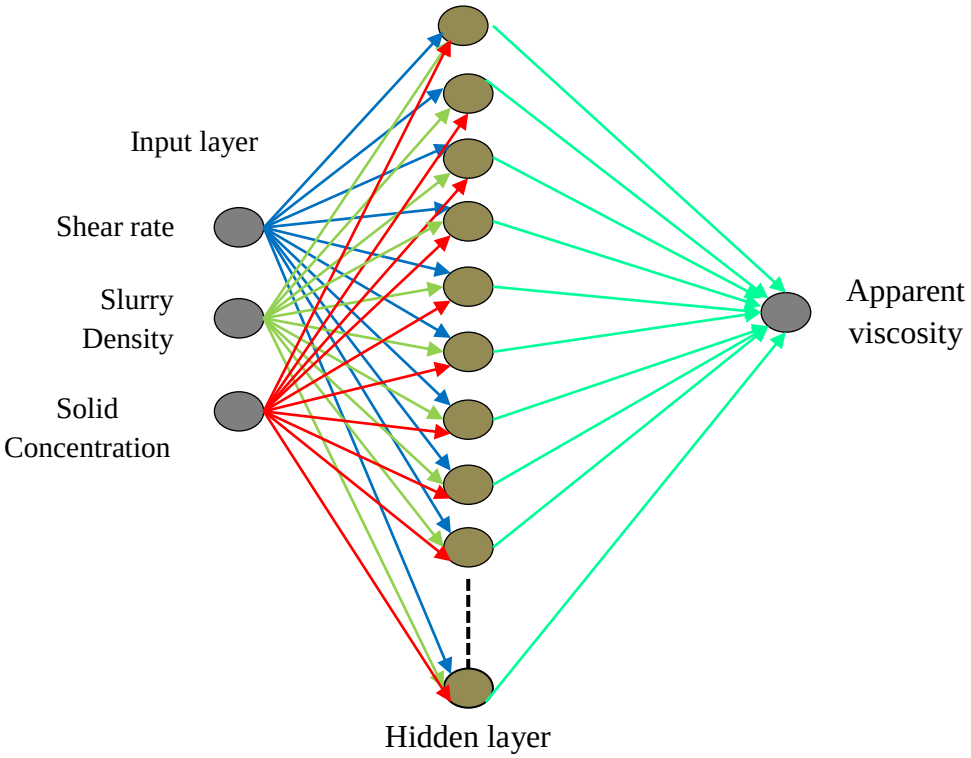

Figure 5.11 3-layered neural network model

Input layer consists of three input neurons namely solid concentration, slurry density and shear rate whereas output layer represents the predicted value of apparent viscosity. Bayesian-Regularization algorithms were utilized to train the neural network due to its fast convergence. To initialize weights layer were generated by using Nguyen-Widrow algorithm and for minimizing errors Back propagation learning rule was applied.

$$dW = \eta \frac{\partial E}{\partial W_{ij}} \tag{7}$$

Where, $\frac{\partial E}{\partial W_{ij}}$ is the error gradient with reference to the weight Wij and η is the learning rate parameter. Term W_{ij} represents the weight update of the link connecting the i^{th} and j^{th} neuron of the two neighboring layers. The training parameters used in prediction of rheology are shown in **Figure 12**. The training and testing functions were normalized in range 0.1-0.9 by using the following equation:

$$y = 0.1 + 0.8\left(\frac{x - x_{\min}}{x_{\max} - x_{\min}}\right) \tag{5.4}$$

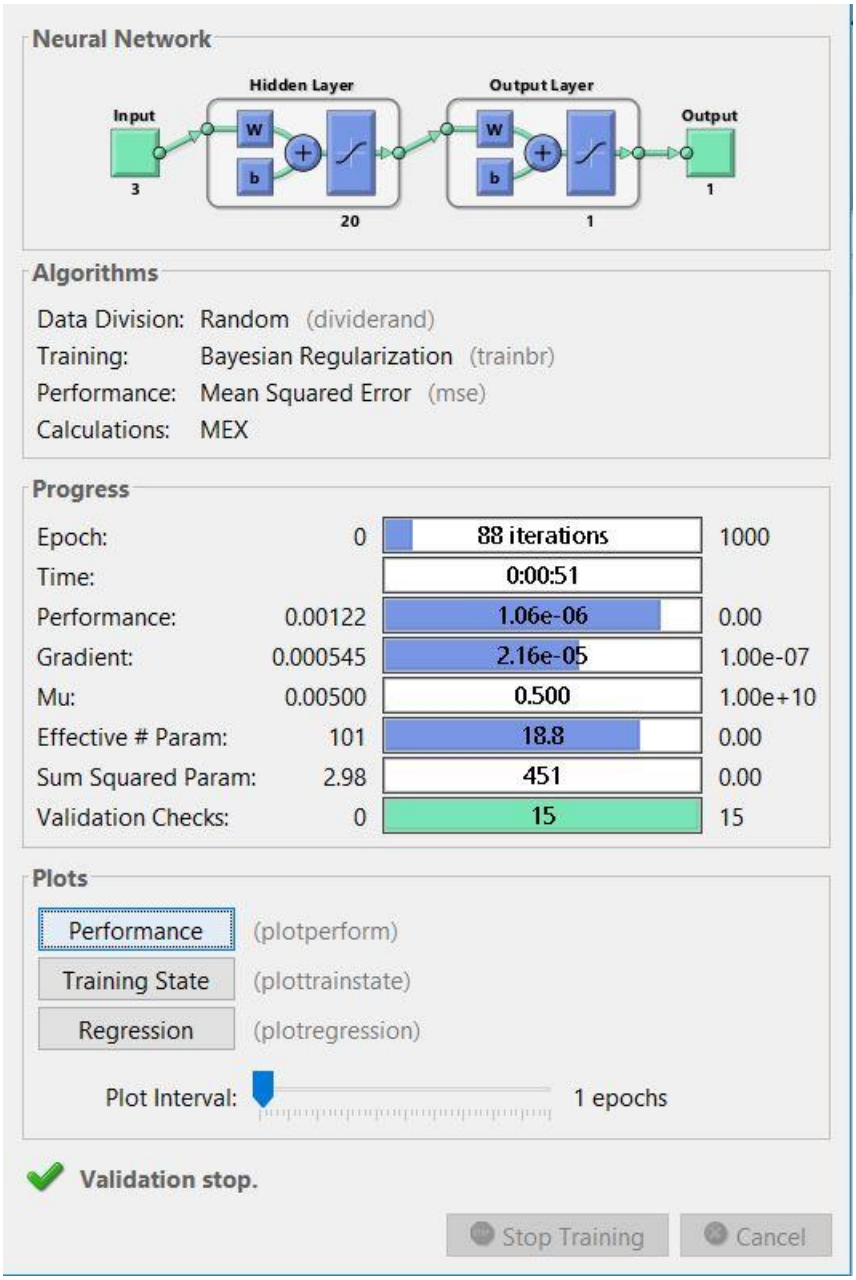

Figure 5.12 . Training parameters used in prediction of apparent viscosity of iron-ore slurry

Root mean square error (RMSE) was used for evaluating the performance between experimental and predicted value. **Figure 13** shows the network performance during the training, testing and validation. For this analysis, total of 20 neurons were taken for training of network. 75% data was used for training, 12.5% data was used for testing and 12.5% data was used for validation.

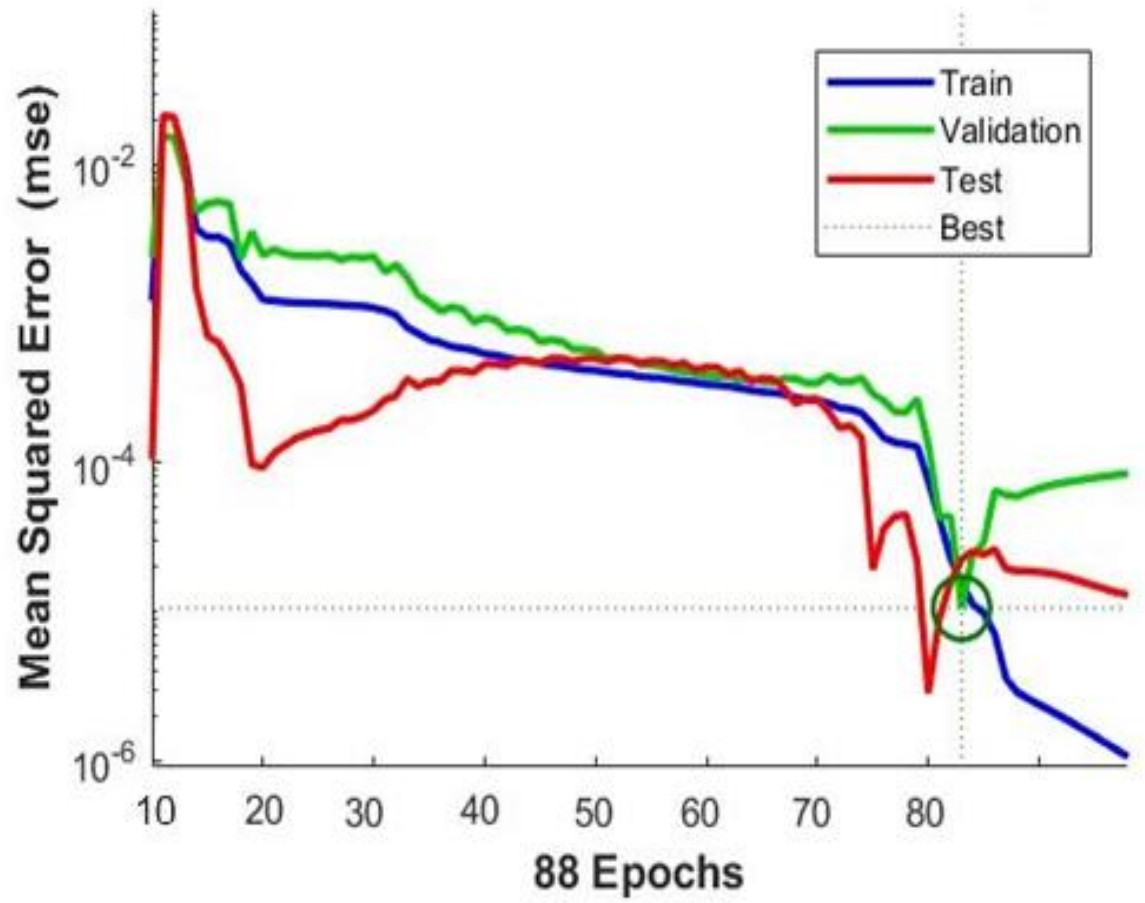

Figure 5.13 Performance graph at time of network training

From Figure 12, the neural network was found to be zero error trained in 88 epochs. Afterwards, the validation of network step was followed for plotting the regression values for training, testing, validation and overall performance. Figure represents the interconnection between network outputs and targets. Regression plots for the prediction of apparent viscosity from ANN model are shown in **Figure 14**. Dashed line represents the targets which discriminate the perfect result and outputs. colored solid lines represent the linear regression fitting line which discriminates between outputs and targets. From Fig. 13, the value of regression coefficient (R^2) for training, testing, validation and performance was found to be best fit and are 0.99868, 0.97941, 0.99955 and 0.99778 respectively. The value of regression coefficient (R^2) was found close to 1 which represents pure linear relationship between outputs and targets.

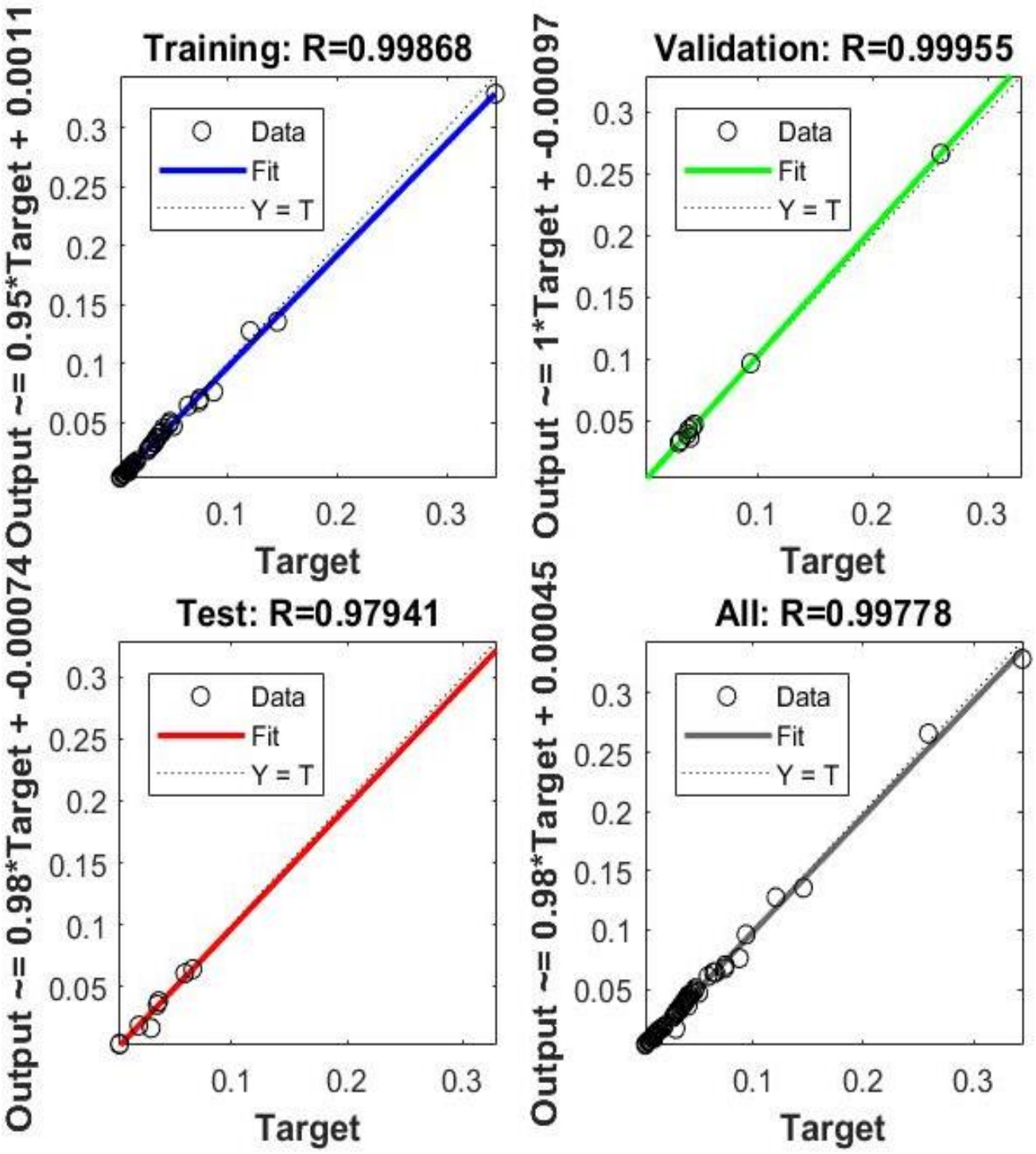

The experimental and ANN predicted viscosity is plotted in Fig. 14. The percentage error between experimental and ANN predicted viscosity was found as ±5% which indicates the close agreement between neural network and experimental results.

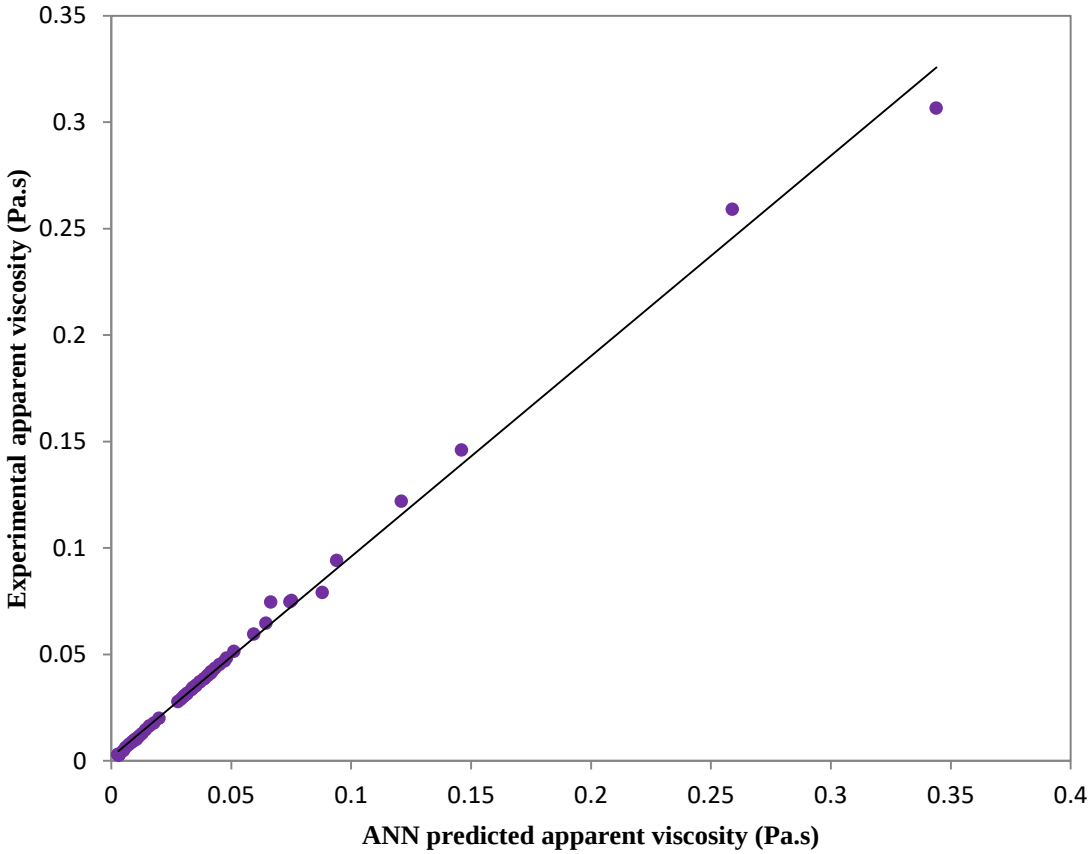

Figure 5.14 Experimental versus ANN prediction graph

Chapter 6

Conclusion

Present study was performed with an objective to examine the physico-chemical and flow behavior of iron-ore and iron-ore water slurry. From present work, it is found that the particle shape and solid concentration highly influenced the flow characteristics of the slurry. To determine the various parameters the simulations were carried out by digital interpretations by reading the pixel and grey value information present in a particular SEM micrograph. The rheoleogical experiments were conducted on Anton Paar rotational rheometer. The following conclusions can be drawn on the basis of present study:

- The particles of sample to be irregular in shape with low value of circularity and sphericity factor. The circularity factor varying from 0.31-0.55 for sample S-1 and 0.30-0.56 for sample S-2. However the value of sphericity was varied 0.34-0.51 and 0.36-0.54 respectively for sample S-1 and S-2.
- The quartz and calcite were found as major crystalline phase along with iron. It was also observed that diffraction intensity is on peaks for quartz and iron present in both samples.
- The viscidness of iron-ore water depends upon the particle size distribution and solid concentration of the slurry. Too coarse particles may settle in pipeline during transportation and also causing pumping problems. Hence a mixture coarse and fine particle can be used for the preparation of slurry as it improves the rheology of slurry.
- The uni-modal slurry shows almost Newtonian behavior at low solid concentration i.e. up to 30% by weight. Further increase in solid loading results non-Newtonian behavior of slurry. Whereas, in case multivariate slurry the flow behavior of slurry is a pesudoplastic even at low solid concentration. The slurry becomes highly pesudoplastic in nature as the solid concentration increases.
- The viscosity of slurry is also depends upon the temperature. With rise in temperature, the viscosity of the slurry falls as owing to the increase in the kinetic energy of carrier fluid which results decrease in the cohesive forces amongst the particles.
- The blending of particles in slurry also improves the flow characteristics. As the optimum ratio of blending for sample S-1 was found to be 30% by weight. Whereas in case of slurry of sample S-2 the optimum value of blending was found to be 20% weight.

Future Scope

The present work was focused on understanding the impact of particle sizes on the morphological and flow (rheological) behavior of iron-ore water slurry. In present work only the influence of particle size at particular solid concentration of slurry, without considering any effect of additives and stabilizers, or increasing the solid loadings has been investigated. The present study can be further extended by adding additives and stabilizers in slurry to improve the flow characteristics. Also the other slurries flow characteristics such as pressure drop, wear analysis can be investigated.

List Publications

Jashanpreet Singh, Satish Kumar*, S. K. Mohapatra, **Sagar Kumar**. Shape simulation of solid particles by digital interpretations of scanning electron micrographs *Materials Today's: proceedings*.

Sagar Kumar, Satish Kumar, Mandeep Singh, Jatinder Pal Singh. Rheological Characteristics of Uni-variant and Bi-variant Particle size distribution of Iron Ore Suspension. *Transactions of the Indian Institute of Metals.: - Under Review*

References

Al-Zahrani, S. M. and Al-Fariss, T. F. (1998) 'A general model for the viscosity of waxy oils', *Chemical Engineering and Processing: Process Intensification*, 37(5), pp. 433–437. doi: 10.1016/S0255-2701(98)00047-6.

Antony N. Beris, A. J. G. (2014) 'Everything Flows', *Applied Rheology*, 24, pp. 1–13. doi: 10.3933/APPLRHEOL-24-52918.

Assefa, K. M. and Kaushal, D. R. (2015) 'Experimental study on the rheological behaviour of coal ash slurries', *Journal of Hydrology and Hydromechanics*, pp. 303–310. doi: 10.1515/johh-2015-0029.

Bobicki, E. R. *et al.* (2013) 'Effect of microwave pre-treatment on grindability of ultramafic nickel ores', *Materials Science and Technology Conference and Exhibition 2013, MS and T 2013*, 3, pp. 97–104.

Chandel, S., Seshadri, V. and Singh, S. N. (2009) 'Effect of additive on pressure drop and rheological characteristics of fly ash slurry at high concentration', *Particulate Science and Technology*, 27(3), pp. 271–284. doi: 10.1080/02726350902922036.

Deosarkar, M. P. and Sathe, V. S. (2012) 'Predicting effective viscosity of magnetite ore slurries by using artificial neural network', *Powder Technology*, 219, pp. 264–270. doi: 10.1016/j.powtec.2011.12.058

G. Vieira, M. and E. C. Peres, A. (2012) 'Effect of Reagents on the Rheological Behavior of an Iron Ore Concentrate Slurry', *International Journal of Mining Engineering and Mineral Processing*, 1(2), pp. 38–42. doi: 10.5923/j.mining.20120102.03.

He, M., Wang, Y. and Forssberg, E. (2004) 'Slurry rheology in wet ultrafine grinding of industrial minerals: A review', *Powder Technology*, pp. 94–112. doi: 10.1016/j.powtec.2004.09.032.

Kissa, E. (1999) *Dispersions : characterization, testing, and measurement*. Available at: https://books.google.com.sg/books?id=0AueaypD1BwC&dq=depletion+flocculation&source=gbs_navlinks_s.

Kumar, K. *et al.* (2017) ‘Measurement of Flow Characteristics for Multiparticulate Bottom Ash-water Suspension with Additives’, *Journal of Residuals Science and Technology*, 14(1), pp. 11–17. doi: 10.12783/issn.1544-8053/14/1/2.

Liu, E. J. *et al.* (2017) ‘Contrasting mechanisms of magma fragmentation during coeval magmatic and hydromagmatic activity: the Hverfjall Fires fissure eruption, Iceland’, *Bulletin of Volcanology*, 79(10). doi: 10.1007/s00445-017-1150-8.

De Lorenzi, L. and Bevilacqua, P. (2002) ‘The influence of particle size distribution and nonionic surfactant on the rheology of coal water fuels produced using Iranian and Venezuelan coals’, *Coal Preparation*, 22(5), pp. 249–268. doi: 10.1080/07349340215012.

Morrison, F. A. (2001) *Understanding Rheology*. Oxford University Press. Inc.

Nguyen, Q. D., Logos, C. and Semmler, T. (1997) ‘Rheological Properties of South Australian Coal-Water Slurries Rheological Properties of South Australian Coal-Water Slurries’, (January 2015), pp. 37–41. doi: 10.1080/07349349708905145.

Nyembwe, A. M., Cromarty, R. D. and Garbers-Craig, A. M. (2017) ‘Relationship Between Iron Ore Granulation Mechanisms, Granule Shapes, and Sinter Bed Permeability’, *Mineral Processing and Extractive Metallurgy Review*, 38(6), pp. 388–402. doi: 10.1080/08827508.2017.1323750.

Roy, S. and Das, A. (2008) ‘Characterization and processing of low-grade iron ore slime from the jilling area of India’, *Mineral Processing and Extractive Metallurgy Review*, 29(3), pp. 213–231. doi: 10.1080/08827500801997886.

Ruiz-Agudo, E. and Rodriguez-Navarro, C. (2010) ‘Microstructure and rheology of lime putty’, *Langmuir*, 26(6), pp. 3868–3877. doi: 10.1021/la903430z.

Sahoo, B. K., De, S. and Meikap, B. C. (2015) ‘An investigation into the influence of microwave energy on iron ore-water slurry rheology’, *Journal of Industrial and Engineering Chemistry*, 25, pp. 122–130. doi: 10.1016/j.jiec.2014.10.022.

Senapati, P. K., Panda, D. and Parida, A. (2009) ‘Predicting Viscosity of Limestone-Water Slurry’, *J. Min. & Mat. Char. & Eng*, 8(3), pp. 203–221. doi: 10.4236/jmmce.2009.83018

Singh, J. P., Kumar, S. and Mohapatra, S. K. (2017) ‘Modelling of two phase solid-liquid

flow in horizontal pipe using computational fluid dynamics technique', *International Journal of Hydrogen Energy*, 42(31), pp. 20133–20137. doi: 10.1016/j.ijhydene.2017.06.060.

Singh, M. K. *et al.* (2016) 'Influence of Particle-Size Distribution and Temperature on Rheological Behavior of Coal Slurry', *International Journal of Coal Preparation and Utilization*, 36(1), pp. 44–54. doi: 10.1080/19392699.2015.1049265.

Singh, J., Kumar, S., Singh, J.P., Kumar, P. and Mohapatra, S.K., 2018. CFD modeling of erosion wear in pipe bend for the flow of bottom ash suspension. *Particulate Science and Technology*, pp.1-11.

Singh, J.P., Kumar, S. and Mohapatra, S.K., 2017. Head Loss Investigations Inside 90° Pipe Bend for Conveying Of Fine Coal–Water Slurry Suspension. *International Journal of Coal Preparation and Utilization*, pp.1-17.

Singh, J.P., Kumar, S. and Mohapatra, S.K., 2017. Modelling of two phase solid-liquid flow in horizontal pipe using computational fluid dynamics technique. *International Journal of Hydrogen Energy*, *42*(31), pp.20133-20137.

'Slurry Tranportation in Indian Mines' (2001). Indian Buearu of Mines.

Tangsathitkulchai, C. (2003) 'The effect of slurry rheology on fine grinding in a laboratory ball mill', *International Journal of Mineral Processing*, 69(1–4), pp. 29–47. doi: 10.1016/S0301-7516(02)00061-3.

Trahana, J. *et al.* (2014) 'Evaluation of pressure drop and particle sphericity for an air-rock bed thermal energy storage system', in *Energy Procedia*, pp. 633–642. doi: 10.1016/j.egypro.2014.10.218.

Vance, K. *et al.* (2013) 'The rheological properties of ternary binders containing Portland cement, limestone, and metakaolin or fly ash', *Cement and Concrete Research*, 52, pp. 196–207. doi: 10.1016/j.cemconres.2013.07.007.

Vieira, M. G. and Peres, A. E. C. (2013) 'Effect of rheology and dispersion degree on the regrinding of an iron ore concentrate', *Journal of Materials Research and Technology*, 2(4), pp. 332–339. doi: 10.1016/j.jmrt.2013.07.002.

Walker, C. I. and Hambe, M. (2015) 'Influence of particle shape on slurry wear of white

iron', *Wear*, 332–333, pp. 1021–1027. doi: 10.1016/j.wear.2014.12.029.

WANG, Y. gang *et al.* (2009) 'Rheological behavior of Shengli coal-solvent slurry at low-temperatures and atmospheric pressure', *Mining Science and Technology*, 19(6), pp. 779–783. doi: 10.1016/S1674-5264(09)60142-3.

Yang, X. and Aldrich, C. (2005) 'Rheology of aqueous magnetite suspensions in uniform magnetic fields', *International Journal of Mineral Processing*, 77(2), pp. 95–103. doi: 10.1016/j.minpro.2005.02.008.

Yavuz, R. and Küçükbayrak, S. (1998) 'Effect of particle size distribution on rheology of lignite-water slurry', *Energy Sources*, 20(9), pp. 787–794. doi: 10.1080/00908319808970098.

Yuchi, W. *et al.* (2005) 'Effects of coal characteristics on the properties of coal water slurry', in *Coal Preparation*, pp. 239–249. doi: 10.1080/07349340500444489.

Zhou, M. *et al.* (2010) 'Rheological behavior investigation of concentrated coal-water suspension', *Journal of Dispersion Science and Technology*, 31(6), pp. 838–843. doi: 10.1080/01932690903333788.